From periodic patterns to quasipatterns

Edgar Knobloch

Department of Physics
University of California, Berkeley, CA 94720, USA

knobloch@berkeley.edu

http://tardis.berkeley.edu

Joint work with A. Archer, A. Rucklidge, P. Subramanian and U. Thiele

Quasicrystals: pattern formation and aperiodic order
ICMS, Edinburgh, 7 June 2018

Outline of talk

- Review of Density Functional Theory and Dynamical Density Functional Theory for soft matter systems
- The Phase Field Crystal model
- Equivariant bifurcation theory and periodic patterns in 2D and 3D
- Crystallization fronts in the PFC model
- Front speed in the PFC model: theory vs (numerical) experiment
- Crystallization fronts in a 1-component GEM-4 model: pushed vs pulled fronts
- Front speed in the GEM-4 model: theory vs (numerical) experiment
- Quasicrystals in 2D and 3D
- Spatially localized quasicrystals in 2D and 3D

Density Functional Theory (DFT)

The free energy of a system of interacting particles is $\mathcal{F}[\rho(\mathbf{r})] =:$

$$k_B T \int d\mathbf{r}\rho(\mathbf{r})[\ln(\Lambda^d \rho(\mathbf{r})) - 1] + \frac{1}{2}\int d\mathbf{r} \int d\mathbf{r}' \rho(\mathbf{r}) v(|\mathbf{r} - \mathbf{r}'|)\rho(\mathbf{r}'),$$

where $v(r)$ is the particle-particle interaction potential. The equilibrium state minimizes the grand potential functional

$$\Omega[\rho(\mathbf{r})] = \mathcal{F}[\rho(\mathbf{r})] + \int d\mathbf{r}\, \rho(\mathbf{r})(\Phi(\mathbf{r}) - \mu),$$

i.e., solves

$$k_B T \ln \rho + \int d\mathbf{r}' v(|\mathbf{r} - \mathbf{r}'|)\rho(\mathbf{r}') + \Phi(\mathbf{r}) - \mu = 0.$$

Here μ is the chemical potential and T the temperature. When $\Phi(\mathbf{r}) = 0$ the resulting ρ can be uniform (liquid) or nonuniform (solid).

Dynamical Density Functional Theory (DDFT)

We assume that under nonequilibrium conditions the particles obey Brownian dynamics

$$\dot{\mathbf{r}}_\ell = -\Gamma \nabla_\ell U(\mathbf{r}_1, \ldots, \mathbf{r}_N) + \Gamma \mathbf{X}_\ell(t),$$

where the index $\ell = 1, ..., N$ labels the particles. The dynamics of such a system can be investigated using Dynamical Density Functional Theory (DDFT):

$$\frac{\partial \rho(\mathbf{r}, t)}{\partial t} = \Gamma \nabla \cdot \left[\rho(\mathbf{r}, t) \nabla \frac{\delta \Omega[\rho(\mathbf{r}, t)]}{\delta \rho(\mathbf{r}, t)} \right],$$

where $\rho(\mathbf{r}, t)$ is the time-dependent nonequilibrium one-body density profile. To derive the DDFT we have used the approximation that the nonequilibrium fluid two-body correlations are the same as those in the equilibrium fluid with the same one-body density distribution.

The DDFT model can be simplified further, resulting in the Phase Field Crystal model (PFC) with order parameter $\phi(\mathbf{r}) \propto \rho(\mathbf{r}) - \rho_0$, with $\phi = \text{const}$ identified with the liquid phase and $\phi \neq \text{const}$ with the solid or crystalline phase.

The Phase Field Crystal model

The Phase Field Crystal (PFC) model is an approximation to DDFT and takes the form

$$\partial_t \phi(\mathbf{x}, t) = \alpha \nabla^2 \frac{\delta F[\phi]}{\delta \phi(\mathbf{x}, t)},$$

where $F[\phi]$ denotes the free energy functional

$$F[\phi] \equiv \int d\mathbf{x} \left[\frac{\phi}{2} [r + (q^2 + \nabla^2)^2] \phi + \frac{\phi^4}{4} \right],$$

$\phi(\mathbf{x}, t)$ is an order parameter field that corresponds to scaled density and α is a (constant) mobility coefficient. It follows that the system evolves according to the equation

$$\partial_t \, \phi \; = \; \alpha \nabla^2 \left[r\phi + (q^2 + \nabla^2)^2 \phi + \phi^3 \right].$$

i.e., the conserved Swift-Hohenberg equation (cSHE).
Steady states solve the fourth order PDE

$$(\nabla^2 + q^2)^2 \phi + r\phi + \phi^3 = \mu.$$

Question: What types of solutions do PDEs of this form admit?

Periodic patterns in two dimensions

Square lattice: we select four wavenumbers from the circle of marginally stable wavenumbers, $\mathbf{k}_1 = \pm k_c(1,0)$, $\mathbf{k}_2 = \pm k_c(0,1)$ and write

$$\phi(x,t) = z_1(t) \exp i\mathbf{k}_1 \cdot \mathbf{x} + z_2(t) \exp i\mathbf{k}_2 \cdot \mathbf{x} + \text{c.c.} + \text{h.o.t.}$$

The symmetry group Γ of the lattice is $D_4 \dot{+} T^2$ and elements of Γ act on the amplitudes (z_1, z_2) as follows:

$$\textbf{translation}: \mathbf{x} \to \mathbf{x} + \mathbf{d}: (z_1, z_2) \to (z_1\, e^{ik_c d_1}, z_2\, e^{ik_c d_2})$$

$$\textbf{reflection}: (z_1, z_2) \to (\bar{z}_1, z_2); \quad \textbf{rotation}: (z_1, z_2) \to (z_2, \bar{z}_1)$$

These operations represent the action of Γ on vectors $(z_1, z_2) \in \mathcal{C}^2$. The equations for the evolution of (z_1, z_2) require that we construct the Hilbert basis of invariant functions and of equivariant vector fields: all invariant scalar functions are of the form $f(\sigma_1, \sigma_2)$, where

$$\sigma_1 = |z_1|^2 + |z_2|^2, \qquad \sigma_2 = (|z_1|^2 - |z_2|^2)^2.$$

Thus

$$(\dot{z}_1, \dot{z}_2) = (f_1(\sigma_1,\sigma_2)z_1 + f_2(\sigma_1,\sigma_2)|z_1|^2 z_1,\, f_3(\sigma_1,\sigma_2)z_2 + f_4(\sigma_1,\sigma_2)|z_2|^2 z_2).$$

Periodic patterns in two dimensions

Here $(f_1, \ldots, f_4)$ are arbitrary real-valued functions of σ_1, σ_2 and λ. Thus

$$\begin{aligned} \dot{z}_1 &= [\lambda + a|z_2|^2 + b(|z_1|^2 + |z_2|^2) + \ldots]z_1, \\ \dot{z}_2 &= [\lambda + a|z_1|^2 + b(|z_1|^2 + |z_2|^2) + \ldots]z_2, \end{aligned}$$

and if $ab \neq 0$, $a + 2b \neq 0$ the coefficients (a, b) completely determine the small amplitude behavior of the solutions (i.e. near the primary bifurcation at $\lambda = 0$). In terms of $(z_1, z_2) = (r_1 \exp i\phi_1, r_2 \exp i\phi_2)$ these equations become

$$\begin{aligned} \dot{r}_1 &= [\lambda + ar_2^2 + b(r_1^2 + r_2^2) + \ldots]r_1, \\ \dot{r}_2 &= [\lambda + ar_1^2 + b(r_1^2 + r_2^2) + \ldots]r_2, \end{aligned}$$

together with $\dot{\phi}_1 = \dot{\phi}_2 = 0$. These equations have the solutions

$$\begin{aligned} &\text{trivial state } (0,0): \\ &\quad \text{stripes } (r,0): \qquad \lambda + ar^2 = 0 \\ &\quad \text{squares } (r,r): \qquad \lambda + (a+2b)r^2 = 0. \end{aligned}$$

One can also calculate the stability of stripes wrt squares and vice versa.

Periodic patterns in two dimensions

Rolls	(R):	$(z_1, z_2) = (r, 0)$	sgn a,	sgn b
Squares	(S):	$(z_1, z_2) = (r, r)$	sgn (2a + b),	$-$sgn b

Thus near $\lambda = 0$ at most one nontrivial state can be stable.

Hexagonal lattice: here we take 6 wavevectors from the circle of marginal stable wavevectors: $\mathbf{k}_1 = k_c(1, 0)$, $\mathbf{k}_{2,3} = k_c(-1, \pm\sqrt{3})/2$. In this case stripes and hexagons bifurcate simultaneously from $\lambda = 0$ and all are unstable:

In this case the most general solution of the linear stability problem takes the form

$$\Theta(x, y, z, t) = \Re\{z_1 e^{ik_e x} + z_2 e^{ik_e(\sqrt{3}y - x)/2} + z_3 e^{-ik_e(\sqrt{3}y + x)/2}\} f_e(z), \tag{13}$$

where $f_e(z)$ is the same function as in (10). The translations now act by

$$\text{translations: } (x, y) \to (x + d_1, y + d_2) : (z_1, z_2, z_3) \to (e^{i\Theta_1} z_1, e^{-i(\Theta_1 + \Theta_2)} z_2, e^{i\Theta_2} z_3),$$

where $\Theta_1 = k_e d_1$, $\Theta_2 = -k_e(\sqrt{3}d_2 + d_1)/2$. The symmetries of the hexagonal unit cell generate the following discrete actions:

$$\begin{aligned}
&\text{rotation through } 2\pi/3 && : (z_1, z_2, z_3) \to (z_2, z_3, z_1),\\
&\text{reflection } (x, y) \to (x, -y) && : (z_1, z_2, z_3) \to (z_1, z_3, z_2),\\
&\text{inversion } (x, y) \to (-x, -y) && : (z_1, z_2, z_3) \to (\overline{z}_1, \overline{z}_2, \overline{z}_3).
\end{aligned}$$

Periodic patterns in two dimensions

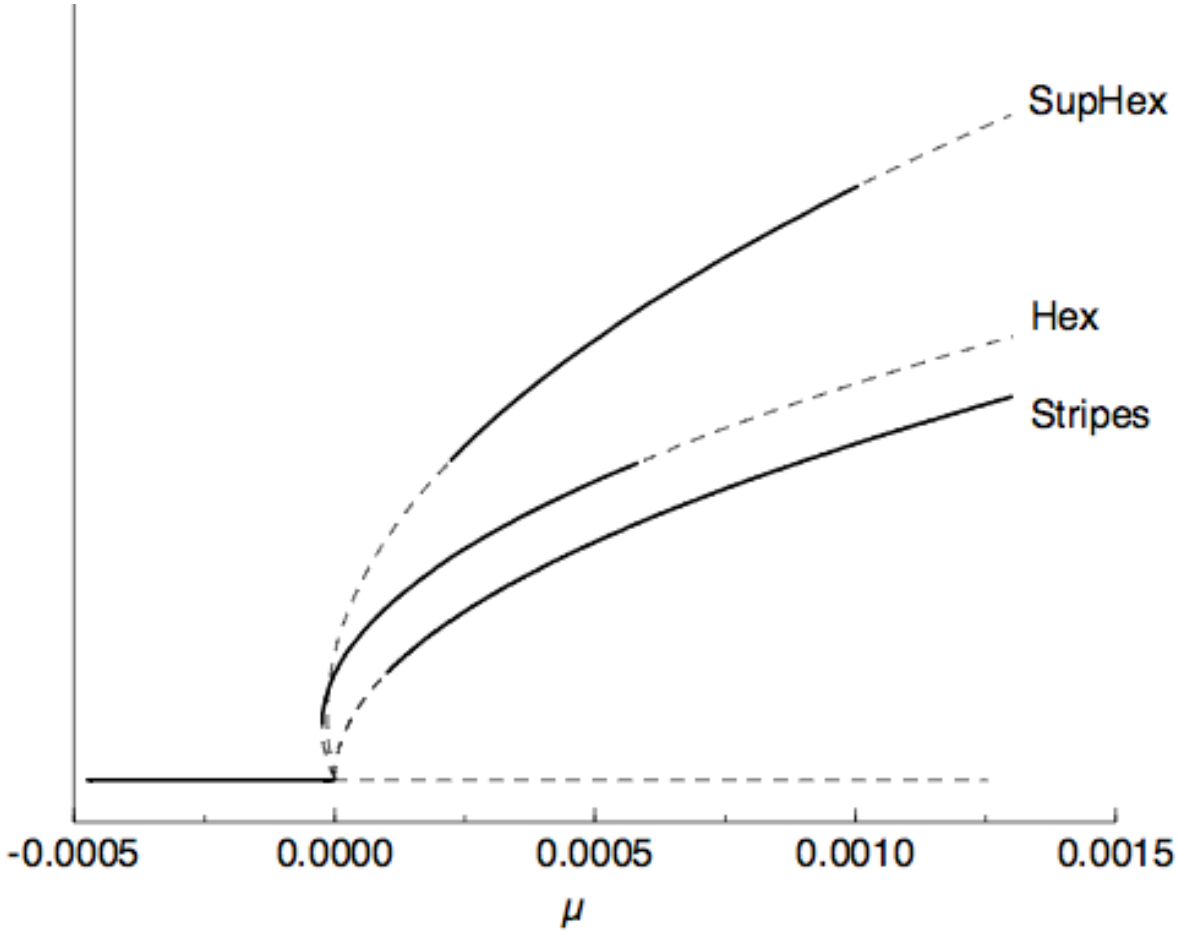

Note the presence of bistability between the hexagons and the trivial state for $\mu < 0$; note also that the stripes for $\mu < 0$ are unstable with respect to hexagonal perturbations. I do not discuss superlattice patterns.

Periodic patterns in three dimensions: cubic lattices

We can extend the above approach to three dimensions. Here I will only describe some results for patterns on a cubic lattice. There are three cases, the simple cubic (SC), the face-centered cubic (FCC), and the body-centered cubic (BCC) lattice corresponding to the choosing 6, 8 or 12 wavevectors from the sphere of marginally stable wavevectors.
For this purpose it is useful to define the isotropy subgroup $\Sigma(\mathbf{z})$ of $\mathbf{z} \in \mathcal{C}^N$:

$$\Sigma(\mathbf{z}) = \{\gamma \in \Gamma \,|\, \gamma \cdot \mathbf{z} = \mathbf{z}\}$$

and the fixed point subspace $\mathrm{Fix}(\Sigma)$ of Σ:

$$\mathrm{Fix}(\Sigma) = \{\mathbf{z} \in \mathcal{C}^N \,|\, \sigma \cdot \mathbf{z} = \mathbf{z} \text{ for all } \sigma \in \Sigma\}.$$

Equivariant Branching Lemma: If $\dim\{\mathrm{Fix}(\Sigma)\} = 1$ then there is a branch of Σ-symmetric solutions that bifurcates from $\mathbf{z} = 0$ at $\lambda = 0$.

Periodic patterns in three dimensions: SC lattice

The SC lattice is generated by the six wavevectors $\pm k_j$, where

$$k_1 = k_c(1,0,0) \qquad k_2 = k_c(0,1,0) \qquad k_3 = k_c(0,0,1) \tag{3.1}$$

relative to Cartesian coordinates (x, y, z). The group Γ acts on $\mathbb{C}^3$ by

$$\tau_\alpha : z_j \to z_j \exp(ik_j \cdot \alpha) \qquad \tau_\alpha \in T^3$$
$$\hat{c} : z_j \to \overline{z}_j \qquad \hat{c} \in \mathbb{Z}_2^c$$

together with the actions of the orientation-preserving symmetries of the cube. These act on the translation invariants $u_j \equiv |z_j|^2$ as the permutation group S_3. The most general vector field commuting with this action of Γ can be written in the form

$$\dot{z}_1 = z_1(h_1 + u_1 h_3 + u_1^2 h_5) \tag{3.2}$$

where each h is an arbitrary real-valued function of the three elementary Γ-invariants σ_1, σ_2, σ_3 and the distinguished bifurcation parameter λ. Here

$$\sigma_1 = u_1 + u_2 + u_3$$
$$\sigma_2 = u_1u_2 + u_2u_3 + u_3u_1$$
$$\sigma_3 = u_1u_2u_3.$$

The equations for $\dot{z}_2$, etc, follow from the requirement of Γ-equivariance. The proof of this

Near $\lambda = 0$ we expand h_1, h_2, h_3 in powers of z. Provided $h_{1,\lambda}(0) \neq 0$, $h_{1,\sigma_1}(0) \neq 0$, $h_3(0) \neq 0$, $h_{1,\sigma_1}(0) + h_3(0) \neq 0$, $2h_{1,\sigma_1}(0) + h_3(0) \neq 0$, $3h_{1,\sigma_1}(0) + h_3(0) \neq 0$ the bifurcation problem is fully determined by the third-order truncation of these equations.

Periodic patterns in three dimensions: SC lattice

Table 1. Symmetry of the primary solution branches on the SC lattice.

Branch	Nomenclature	Symmetry Σ	Fix(Σ)
0	Trivial	$T^3 \dot{+} \mathbb{O} \oplus \mathbb{Z}_2^c$	$(0,0,0)$
I	Lamellae	$T^2 \dot{+} \mathbb{D}_4 \oplus \mathbb{Z}_2^c$	$(x,0,0)$
II	Square prism	$T \dot{+} \mathbb{D}_4 \oplus \mathbb{Z}_2^c$	$(x,x,0)$
III	Simple cubic	$\mathbb{O} \oplus \mathbb{Z}_2^c$	(x,x,x)

Table 2. The primary solution branches on the SC lattice.

Branch	(z_1, z_2, z_3)	σ_1	Branching equation
0	$(0,0,0)$	0	$\sigma_1 = 0$
I	$(x,0,0)$	x^2	$h_{1,\lambda}\lambda + (h_{1,\sigma_1} + h_3)\sigma_1 = \mathrm{O}(4)$
II	$(x,x,0)$	$2x^2$	$h_{1,\lambda}\lambda + \frac{1}{2}(2h_{1,\sigma_1} + h_3)\sigma_1 = \mathrm{O}(4)$
III	(x,x,x)	$3x^2$	$h_{1,\lambda}\lambda + \frac{1}{3}(3h_{1,\sigma_1} + h_3)\sigma_1 = \mathrm{O}(4)$

Periodic patterns in three dimensions: SC lattice

Table 3. The eigenvalues of the solution branches on the SC lattice.

Branch	Eigenvalues	Comment
0	λ (6 times)	
I	$h_{1,\sigma_1} + h_3, -h_3$ (4 times), 0 (once)	
II	$2h_{1,\sigma_1} + h_3, h_3, h_{1,\sigma_1}, h_3, -h_3, 0$ (twice)	Always unstable
III	$3h_{1,\sigma_1} + h_3, h_3$ (twice), 0 (3 times)	

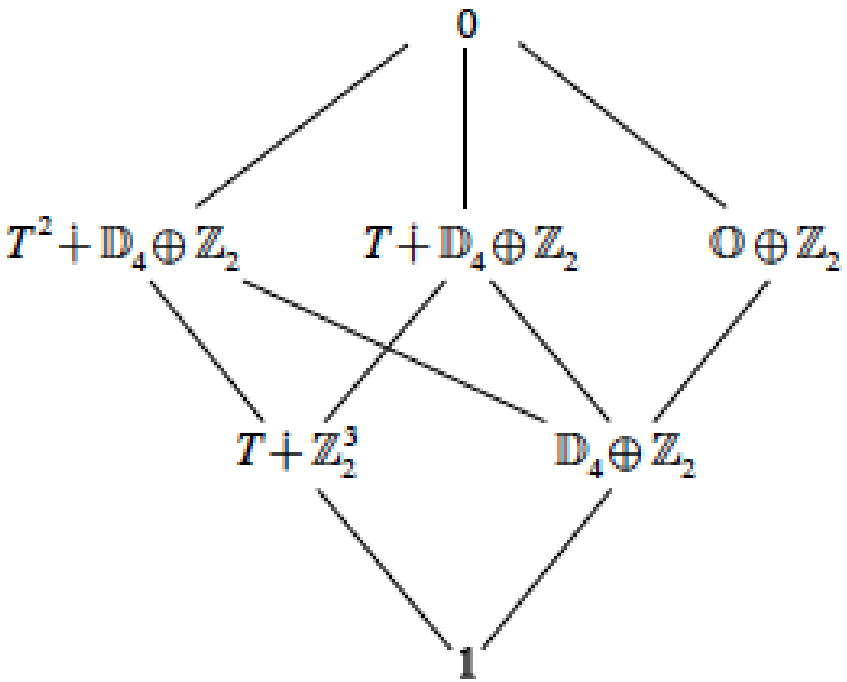

Periodic patterns in three dimensions: FCC lattice

The FCC lattice is generated by the eight wavevectors $\pm k_j$, where

$$k_1 = \frac{k_c}{\sqrt{3}}(1,1,1) \qquad k_2 = \frac{k_c}{\sqrt{3}}(1,-1,-1)$$
$$k_3 = \frac{k_c}{\sqrt{3}}(-1,1,-1) \qquad k_4 = \frac{k_c}{\sqrt{3}}(-1,-1,1).$$

As in the case of the SC lattice we seek the most general vector field that commutes with the appropriate action of the group Γ. We obtain

$$\dot{z}_1 = z_1(h_1 + u_1 h_3 + u_1^2 h_5 + u_1^3 h_7) + \overline{z}_2\overline{z}_3\overline{z}_4(p_3 + u_1 p_5 + u_1^2 p_7 + u_1^3 p_9) \tag{4.1}$$

where each h and p is an arbitrary real-valued function of the five elementary Γ-invariants $\sigma_1, \sigma_2, \sigma_3, \sigma_4, q$ and the distinguished bifurcation parameter λ. Here

$$\sigma_1 = u_1 + u_2 + u_3 + u_4$$
$$\sigma_2 = u_1u_2 + u_1u_3 + u_1u_4 + u_2u_3 + u_2u_4 + u_3u_4$$
$$\sigma_3 = u_1u_2u_3 + u_1u_2u_4 + u_1u_3u_4 + u_2u_3u_4$$
$$\sigma_4 = u_1u_2u_3u_4$$
$$q = z_1z_2z_3z_4 + \overline{z}_1\overline{z}_2\overline{z}_3\overline{z}_4$$

and, as before, $u_j = |z_j|^2$ (see appendix A). The equations for $\dot{z}_2$, etc, again follow from the requirement of Γ-equivariance. The resulting equations form a special case of those studied in reference [13].

Periodic patterns in three dimensions: FCC lattice

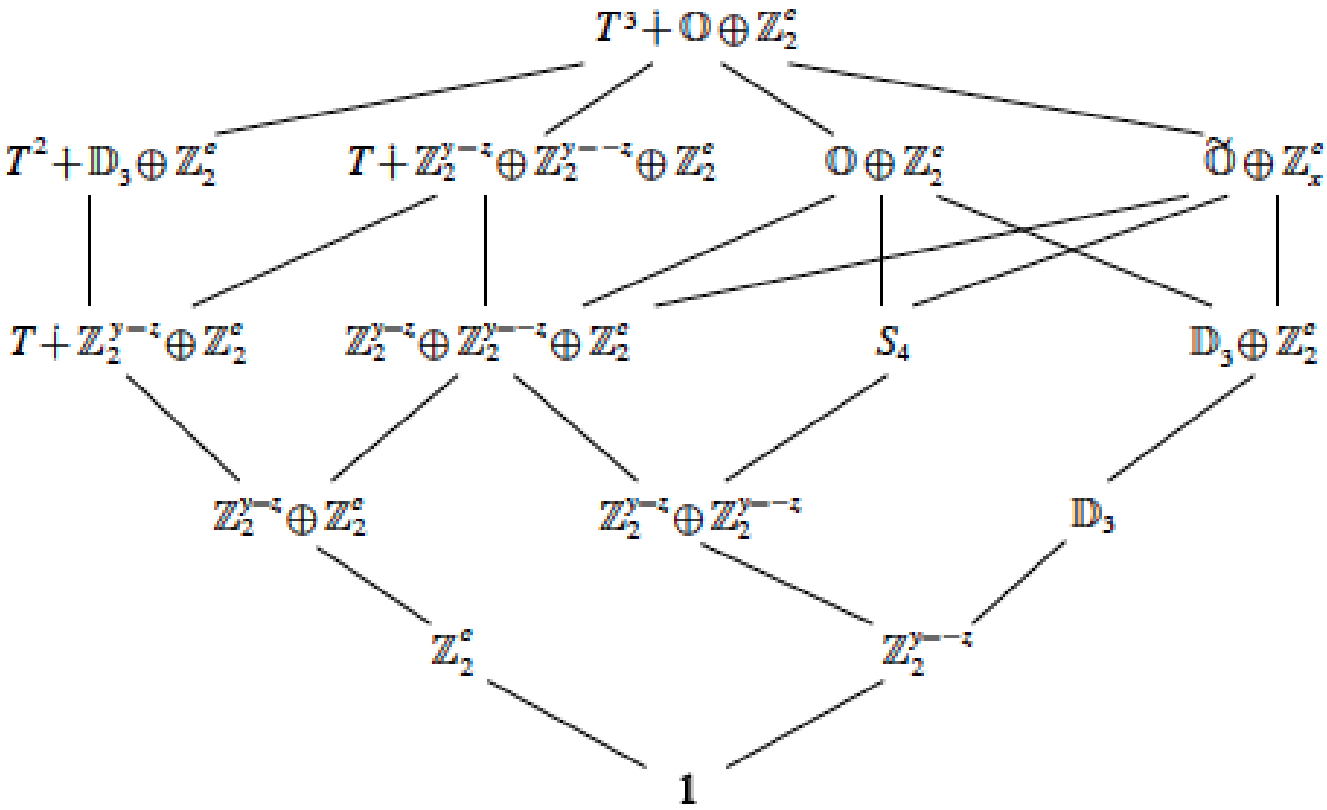

Figure 2. Lattice of isotropy subgroups for the FCC lattice.

Callahan and Knobloch, Nonlinearity **10**, 1179–1206 (1997)

Periodic patterns in three dimensions: FCC lattice

Table 4. Symmetry of the primary solution branches on the FCC lattice.

Branch	Nomenclature	Symmetry Σ	Fix(Σ)
0	Trivial	$T^3 \dot{+} \mathbb{O} \oplus \mathbb{Z}_2^c$	$(0,0,0,0)$
I	Lamellae	$T^2 \dot{+} \mathbb{D}_3 \oplus \mathbb{Z}_2^c$	$(x,0,0,0)$
II	Rhombohedral	$T^1 \dot{+} \mathbb{Z}_2^{y=z} \oplus \mathbb{Z}_2^{y=-z} \oplus \mathbb{Z}_2^c$	$(x,x,0,0)$
III$^+$	Face-centred cubic	$\mathbb{O} \oplus \mathbb{Z}_2^c$	(x,x,x,x)
III$^-$	Double-diamond	$\tilde{\mathbb{O}} \oplus \mathbb{Z}_2^c$	$(-x,x,x,x)$
IV	Submaximal	$\mathbb{D}_3 \oplus \mathbb{Z}_2^c$	(x,x,x,y)

Callahan and Knobloch, Nonlinearity **10**, 1179–1206 (1997)

Periodic patterns in three dimensions: FCC lattice

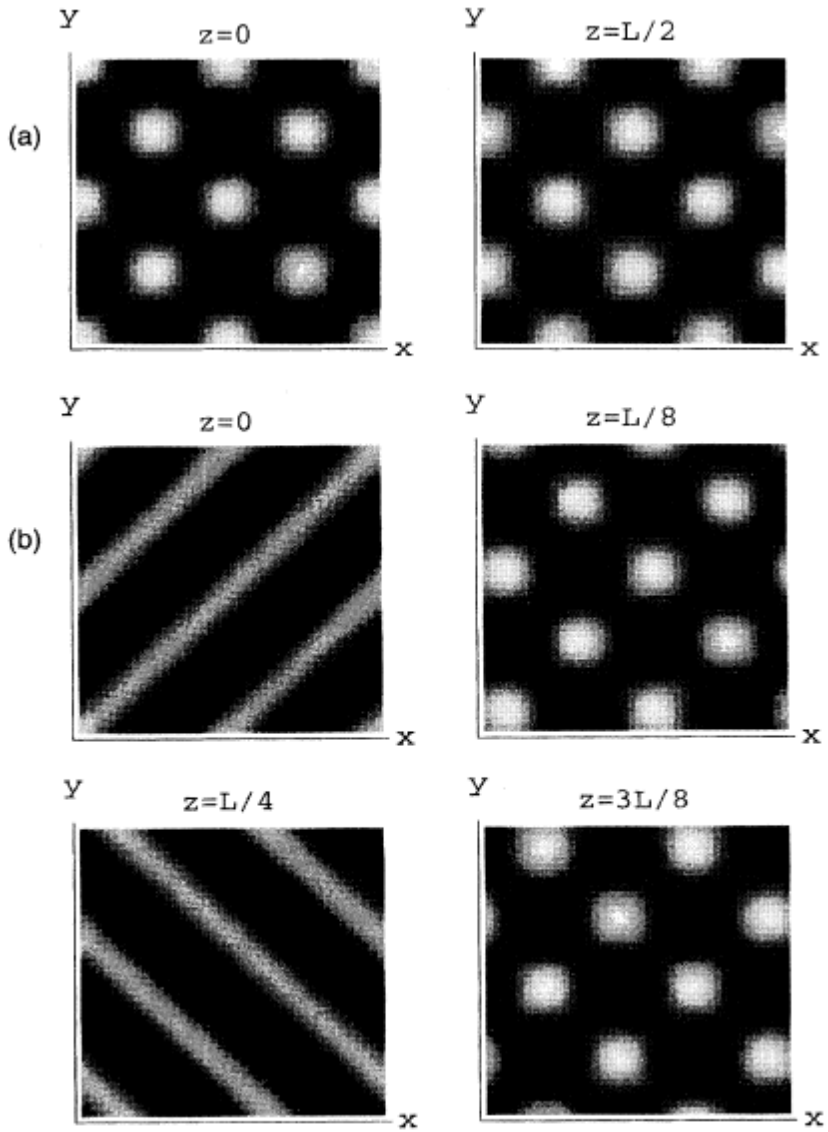

FIG. 1. The (a) fcc and (b) double-diamond solutions shown by means of horizontal sections. The grey scale indicates the magnitude of $X(\mathbf{x})$, with white denoting maximum and black minimum.

Periodic patterns in three dimensions: FCC lattice

Table 5. The primary solution branches on the FCC lattice.

Branch	(z_1, z_2, z_3, z_4)	σ_1	Branching equation
0	$(0,0,0,0)$	0	$\sigma_1 = 0$
I	$(x,0,0,0)$	x^2	$h_{1,\lambda}\lambda + (h_{1,\sigma_1} + h_3)\sigma_1 = \mathrm{O}(4)$
II	$(x,x,0,0)$	$2x^2$	$h_{1,\lambda}\lambda + \frac{1}{2}(2h_{1,\sigma_1} + h_3)\sigma_1 = \mathrm{O}(4)$
III$^+$	(x,x,x,x)	$4x^2$	$h_{1,\lambda}\lambda + \frac{1}{4}(4h_{1,\sigma_1} + h_3 + p_3)\sigma_1 = \mathrm{O}(4)$
III$^-$	$(-x,x,x,x)$	$4x^2$	$h_{1,\lambda}\lambda + \frac{1}{4}(4h_{1,\sigma_1} + h_3 - p_3)\sigma_1 = \mathrm{O}(4)$
IV	(x,x,x,y)	$3x^2 + y^2$	$y = (p_3/h_3)x$, $h_{1,\lambda}\lambda + (3h_{1,\sigma_1} + h_3)x^2 + (h_{1,\sigma_1} + h_3)y^2 = \mathrm{O}(4)$

$h_1(0) = 0$, $h_{1,\lambda}(0) \neq 0$, the non-degeneracy conditions

$$h_3 \neq 0 \qquad p_3 \neq 0 \qquad h_{1,\sigma_1} + h_3 \neq 0 \qquad 2h_{1,\sigma_1} + h_3 \neq 0$$
$$4h_{1,\sigma_1} + h_3 \pm p_3 \neq 0 \qquad h_3 \pm p_3 \neq 0 \qquad (3h_{1,\sigma_1} + h_3)h_3^2 + (h_{1,\sigma_1} + h_3)p_3^2 \neq 0. \tag{4.2}$$

Here, and in the following, it is understood that all quantities are evaluated at $\lambda = \sigma_1 = \sigma_2 = \sigma_3 = \sigma_4 = q = 0$. With these hypotheses the solution branches and their stability properties are determined by the truncation at third order of equations (4.1). The resulting

Callahan and Knobloch, Nonlinearity **10**, 1179–1206 (1997)

Periodic patterns in three dimensions: FCC lattice

4.1. Remark on stability calculations

The isotropy subgroup structure can greatly facilitate the computation of the linearized (orbital) stability of the solutions, cf [1, 10]. This is because the Jacobian, Df, of equations (4.1) linearized about a non-trivial equilibrium, z, must commute with every element $\sigma \in \Sigma(z)$. Take, for example, the fcc branch III$^+$, with $\Sigma = \mathbb{O} \oplus \mathbb{Z}_2^c$. Let us represent the vector z in the real basis $(x_1, x_2, x_3, x_4, y_1, y_2, y_3, y_4)$. The fact that Df commutes with $\mathbb{Z}_2^c$ implies that Df must be of the form

$$Df = \begin{pmatrix} \mathbf{P} & 0 \\ 0 & \mathbf{Q} \end{pmatrix}$$

for some real matrices $\mathbf{P}$ and $\mathbf{Q}$. The fact that Df commutes with the permutation group $S_4 \subset \mathbb{O}$ implies that $\mathbf{P}$ and $\mathbf{Q}$ have the form

$$\mathbf{P} = \begin{pmatrix} A & B & B & B \\ B & A & B & B \\ B & B & A & B \\ B & B & B & A \end{pmatrix} \qquad \mathbf{Q} = \begin{pmatrix} C & D & D & D \\ D & C & D & D \\ D & D & C & D \\ D & D & D & C \end{pmatrix}.$$

We also know that there are three null eigenvectors corresponding to translations of the solution. An infinitesimal translation in the $\hat{x}$ direction adds an infinitesimal imaginary part $(0, 0, 0, 0, \delta, \delta, -\delta, -\delta)$ to our solution $(x, x, x, x, 0, 0, 0, 0)$. The fact that this gives us a null eigenvalue implies that $C = D$. The eigenvalues of Df must therefore be $A + 3B$ (once), $A - B$ (3 times), $4C$ (once) and 0 (3 times), where

$$A = \frac{\partial \dot{x}_1}{\partial x_1} = \tfrac{1}{4}[2h_{1,\sigma_1} + 2h_3 - p_3]\sigma_1 + \mathrm{O}(\sigma_1^2)$$

$$B = \frac{\partial \dot{x}_1}{\partial x_2} = \tfrac{1}{4}[2h_{1,\sigma_1} + p_3]\sigma_1 + \mathrm{O}(\sigma_1^2)$$

$$C = \frac{\partial \dot{y}_1}{\partial y_1} = -p_3\sigma_1 + \mathrm{O}(\sigma_1^2).$$

Periodic patterns in three dimensions: FCC lattice

Table 6. The eigenvalues of the solution branches on the FCC lattice, and the regions of figure 4 where stable branches exist. (**Bold** means stable for $h_3 < 0$, roman means stable for $h_3 > 0$.)

Branch	Eigenvalues	Regions of stability
0	λ (8 times)	All
I	$h_{1,\sigma_1} + h_3, -h_3$ (6 times), 0 (once)	A, B, C, D, E, F
II	$2h_{1,\sigma_1} + h_3, h_3, -(h_3 \pm p_3)$ (twice each), 0 (twice)	$\emptyset$
III$^+$	$4h_{1,\sigma_1} + h_3 + p_3, -p_3, h_3 - p_3$ (3 times), 0 (3 times)	B, G, **K**, **L**
III$^-$	$4h_{1,\sigma_1} + h_3 - p_3, +p_3, h_3 + p_3$ (3 times), 0 (3 times)	E, H, **I**, **J**
IV	$(3h_{1,\sigma_1} + h_3)x^2 + (h_{1,\sigma_1} + h_3)y^2, h_3(h_3^2 - p_3^2)$ (twice), $-h_3(h_3^2 - p_3^2), -h_3, 0$ (3 times)	$\emptyset$

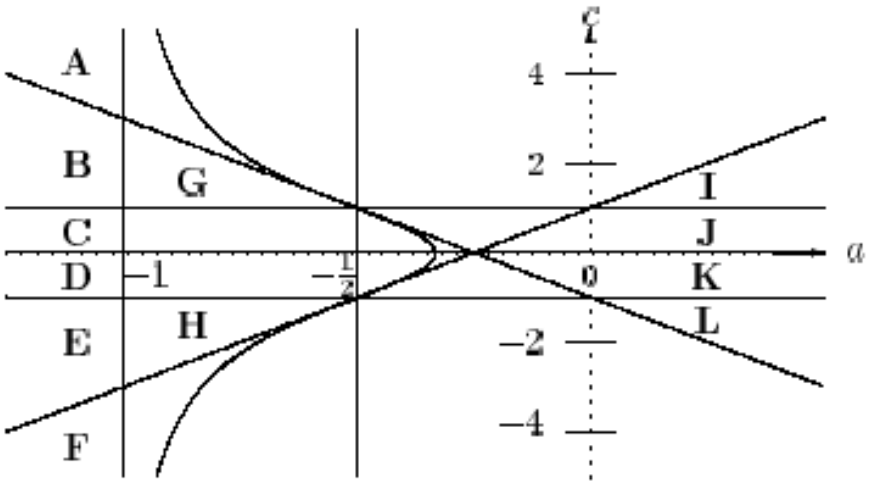

Figure 4. The (a, c) plane showing the regions with different bifurcation diagrams for the FCC lattice.

Periodic patterns in three dimensions: FCC lattice

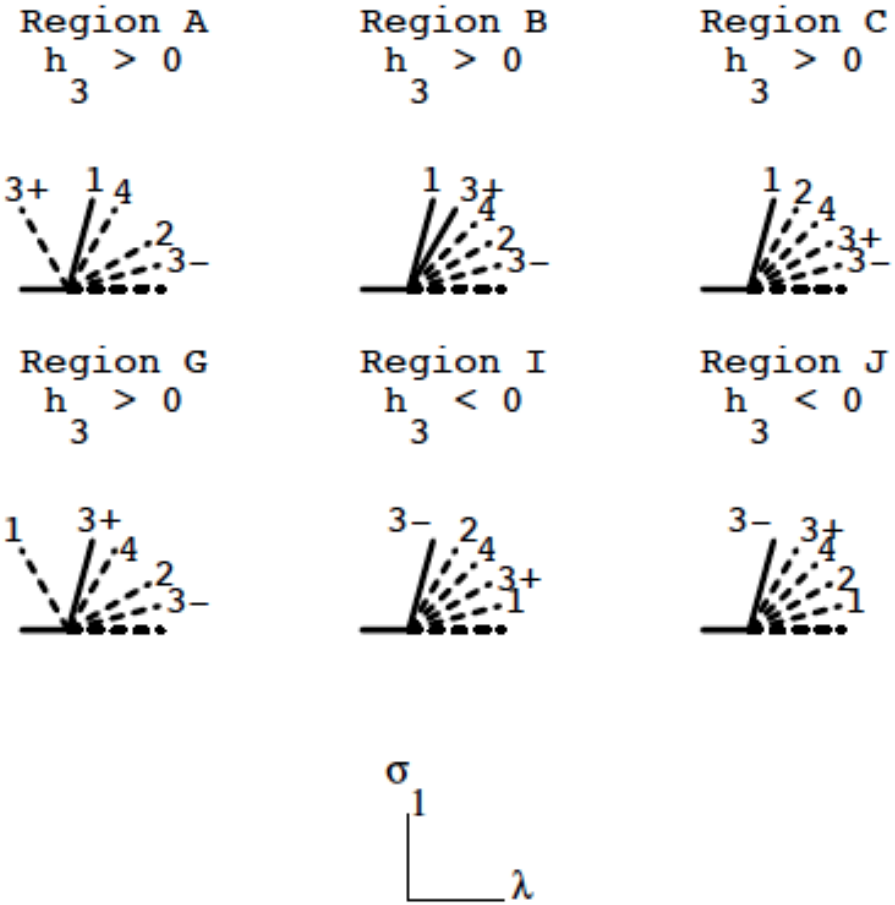

Figure 5. The six bifurcation diagrams σ_1 versus λ (with $c > 0$) containing stable solutions, labelled by region. The stable branches are denoted by a full line. In regions B and I of figure 4 the relative amplitude of branches 1 and 3^+ depends upon c. We assume in these cases that $1 < c < 3$. For $c < 0$ the diagrams are the same, but with the labels 3^+ and 3^- interchanged.

Periodic patterns in three dimensions: BCC lattice

The BCC lattice is generated by the 12 wavevectors $\pm k_j$, where

$$k_1 = \frac{k_c}{\sqrt{2}}(1,1,0) \qquad k_2 = \frac{k_c}{\sqrt{2}}(0,1,1) \qquad k_3 = \frac{k_c}{\sqrt{2}}(1,0,1)$$

$$k_4 = \frac{k_c}{\sqrt{2}}(1,-1,0) \qquad k_5 = \frac{k_c}{\sqrt{2}}(0,1,-1) \qquad k_6 = \frac{k_c}{\sqrt{2}}(-1,0,1).$$

The most general system which commutes with the appropriate action of the group Γ is, to third order,

$$\begin{aligned}\dot{z}_1 = \lambda z_1 + \tfrac{1}{2}a_{12}(z_3 z_5 + z_2\bar{z}_6) + a_1|z_1|^2 z_1 + a_8|z_4|^2 z_1 + \tfrac{1}{2}a_{16}(z_2 z_4 z_5 + z_3\bar{z}_4\bar{z}_6) \\ + \tfrac{1}{4}a_3(|z_2|^2 + |z_3|^2 + |z_5|^2 + |z_6|^2)z_1 + \mathrm{O}(z^4) \qquad (5.1)\end{aligned}$$

with 11 additional equations generated from (5.1) by applying appropriate elements in Γ.

Periodic patterns in three dimensions: BCC lattice

Table 7. The maximal isotropy branches on the BCC lattice with the extra reflection symmetry $\mathbb{Z}_2(-I)$. Here x is real.

Branch	$(z_1, \ldots, z_6)$	Solution
Trivial	$(0,0,0,0,0,0)$	
Lamellae	$(x,0,0,0,0,0)$	$\lambda = -a_1 x^2$
Rhombs	$(x,x,0,0,0,0)$	$\lambda = -(a_1 + \frac{1}{4}a_3)x^2$
Squares	$(x,0,0,x,0,0)$	$\lambda = -(a_1 + a_8)x^2$
Hexes	$(0,0,0,x,x,x)$	$\lambda = -(a_1 + \frac{1}{2}a_3)x^2$
Triangles	$\mathrm{i}(0,0,0,x,x,x)$	$\lambda = (a_1 + \frac{1}{2}a_3)x^2$
bcc	(x,x,x,x,x,x)	$\lambda = -(a_1 + a_{16} + a_3 + a_8)x^2$
bccI	$\mathrm{i}(x,x,x,x,x,x)$	$\lambda = (a_{16} - a_1 - a_3 - a_8)x^2$
123	$(x,x,x,0,0,0)$	$\lambda = -(a_1 + \frac{1}{2}a_3)x^2$
A	$(0,x,x,0,-x,x)$	$\lambda = (-a_1 + \frac{1}{2}a_{16} + \frac{1}{2}a_3 + a_8)x^2$
B	$\lambda = (0,x,x,0,x,x)$	$(a_1 + \frac{1}{2}a_{16} + \frac{1}{2}a_3 + a_8)x^2$

Callahan and Knobloch, Nonlinearity **10**, 1179–1206 (1997)

Periodic patterns in three dimensions: BCC lattice

Table 8. The eigenvalues, with positive prefactors removed, of the solutions listed in table 7.

Branch	Eigenvalues
Trivial	λ (12 times)
Lamellae	0, a_1, $a_8 - a_1$ (twice), $a_3 - 4a_1$ (8 times)
Rhombs	0 (twice), $4a_1 - a_3$, $-4a_1 + a_3$ (3 times), $4a_1 + a_3$ (twice), $-2a_1 - a_{16} + 2a_8$ (4 times)
Squares	0 (twice), $-2a_1 - a_{16} + a_3 - 2a_8$ (4 times), $a_1 - a_8$, $a_1 + a_8$ $-2a_1 + a_{16} + a_3 - 2a_8$ (4 times),
Hexes	0 (twice), $-a_{23}$, $4a_1 - a_3$ (twice), $2a_1 + a_3$, $-a_1 + a_{16} + a_8$ (twice), $-2a_1 - a_{16} + 2a_8$ (4 times)
Triangles	0 (twice), a_{23}, $4a_1 - a_3$ (twice), $2a_1 + a_3$, $-a_1 - a_{16} + a_8$ (twice), $-2a_1 + a_{16} + 2a_8$ (4 times)
bcc	0 (3 times), $-a_{16}$ (3 times), $a_1 - a_{16} - a_8$ (3 times), $2a_1 - a_{16} - a_3 + 2a_8$ (twice),$a_1 + a_{16} + a_3 + a_8$,
bccI	0 (3 times), a_{16} (3 times), $a_1 + a_{16} - a_8$ (3 times), $a_1 - a_{16} + a_3 + a_8$, $2a_1 + a_{16} - a_3 + 2a_8$ (twice)
123	0 (3 times), $4a_1 - a_3$ (twice), $2a_1 + a_3$, $-a_1 - a_{16} + a_8$, $-a_1 + a_{16} + a_8$, $-2a_1 - a_{16} + 2a_8$ (twice), $-2a_1 + a_{16} + 2a_8$ (twice)
A	0 (3 times), a_{16}, $2a_1 + a_{16} - 2a_8$ (twice), $-2a_1 - a_{16} + a_3 - 2a_8$, $-2a_1 + a_{16} + a_3 - 2a_8$ (twice), $-2a_1 + 3a_{16} + a_3 - 2a_8$, $2a_1 + a_{16} - a_3 + 2a_8$, $2a_1 - a_{16} + a_3 + 2a_8$
B	0 (3 times), a_{16}, $-2a_1 - a_{16} - a_3 - 2a_8$, $-2a_1 + a_{16} + a_3 - 2a_8$, $-2a_1 + a_{16} + 2a_8$ (twice), $2a_1 - a_{16} - a_3 + 2a_8$, $2a_1 + a_{16} - a_3 + 2a_8$ (twice), $2a_1 + 3a_{16} - a_3 + 2a_8$

Callahan and Knobloch, Nonlinearity **10**, 1179–1206 (1997)

Periodic patterns in three dimensions: BCC lattice

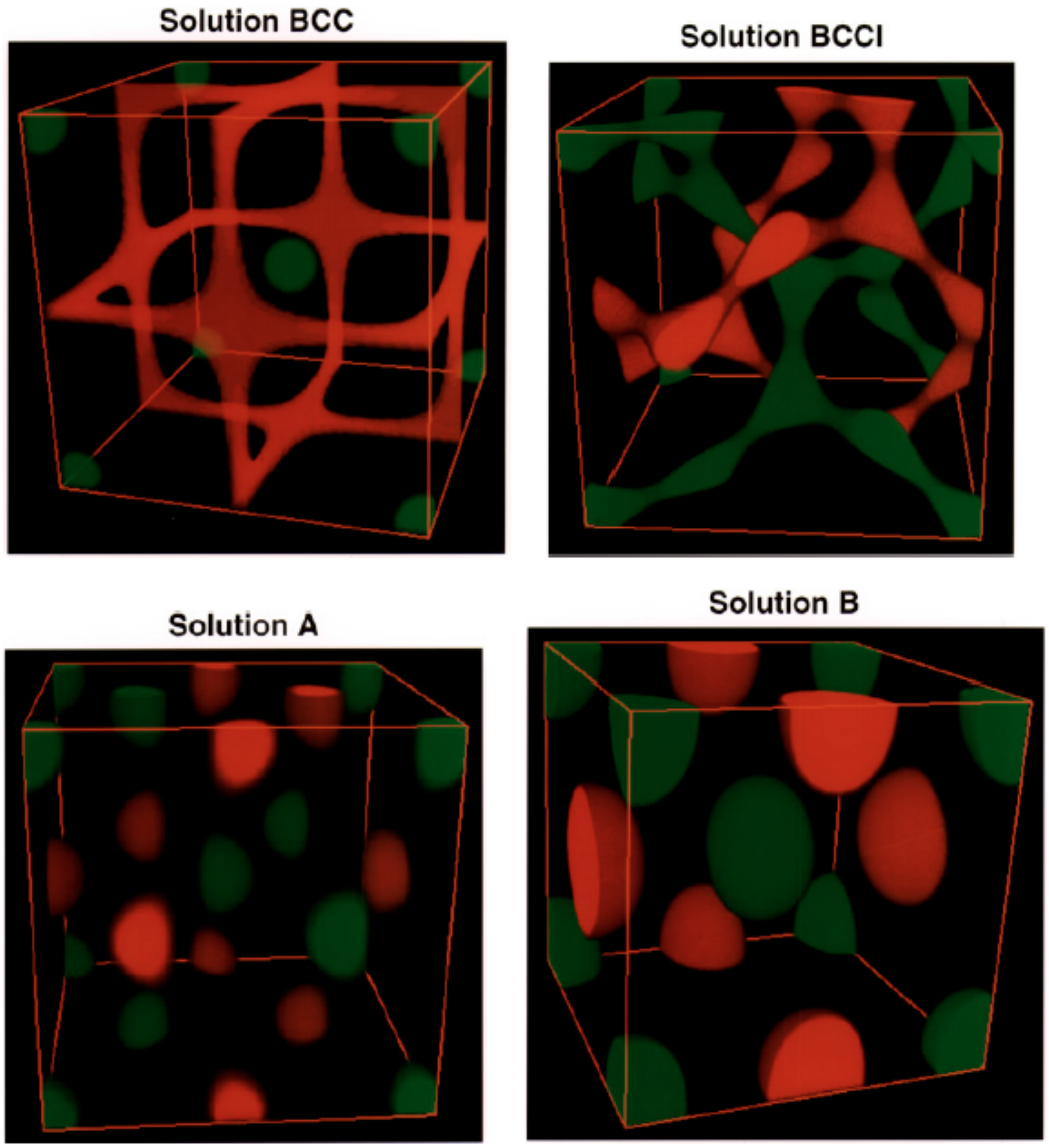

Wavelength selection

The observed wavelength is limited by a number of secondary instabilities. The simplest is the Eckhaus instability. For stripes near onset we have

$$A_t = \mu A + A_{xx} - |A|^2 A$$

with steady solution $A = \sqrt{\mu - Q^2}\exp iQx$. Hence $\mu > Q^2$. Perturbations $a(x,t) = [\alpha(t)\exp i\xi x + \beta(t)\exp -i\xi x]\exp iQx$ are stable if $\mu > 3Q^2 - (1/2)\xi^2$ but unstable otherwise:

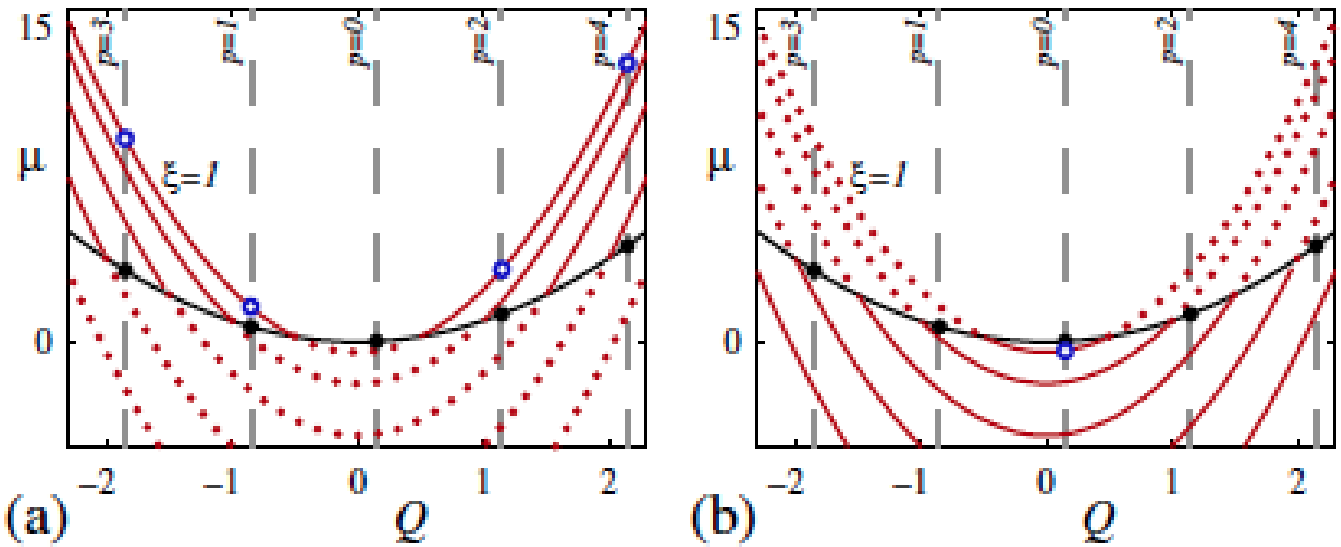

In conserved systems the wavenumber k that minimizes the free energy differs for each state.

Snaking in two spatial dimensions: SH23

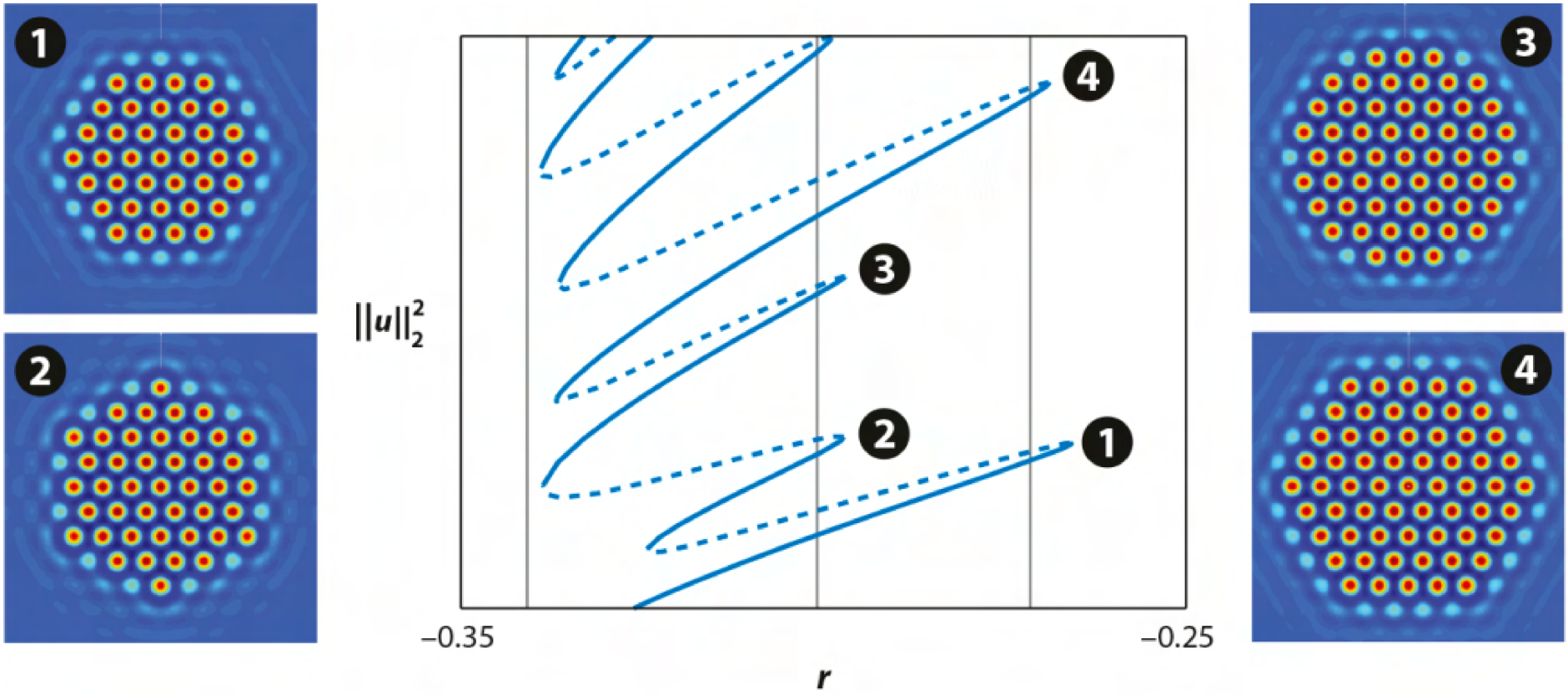

Lloyd et al., SIADS **7**, 1049–1100 (2008)

Review: Knobloch, Annu. Rev. Cond. Matter Phys. **6**, 325–359 (2015)

DFT for a GEM-4 fluid in 2D: Equilibrium front

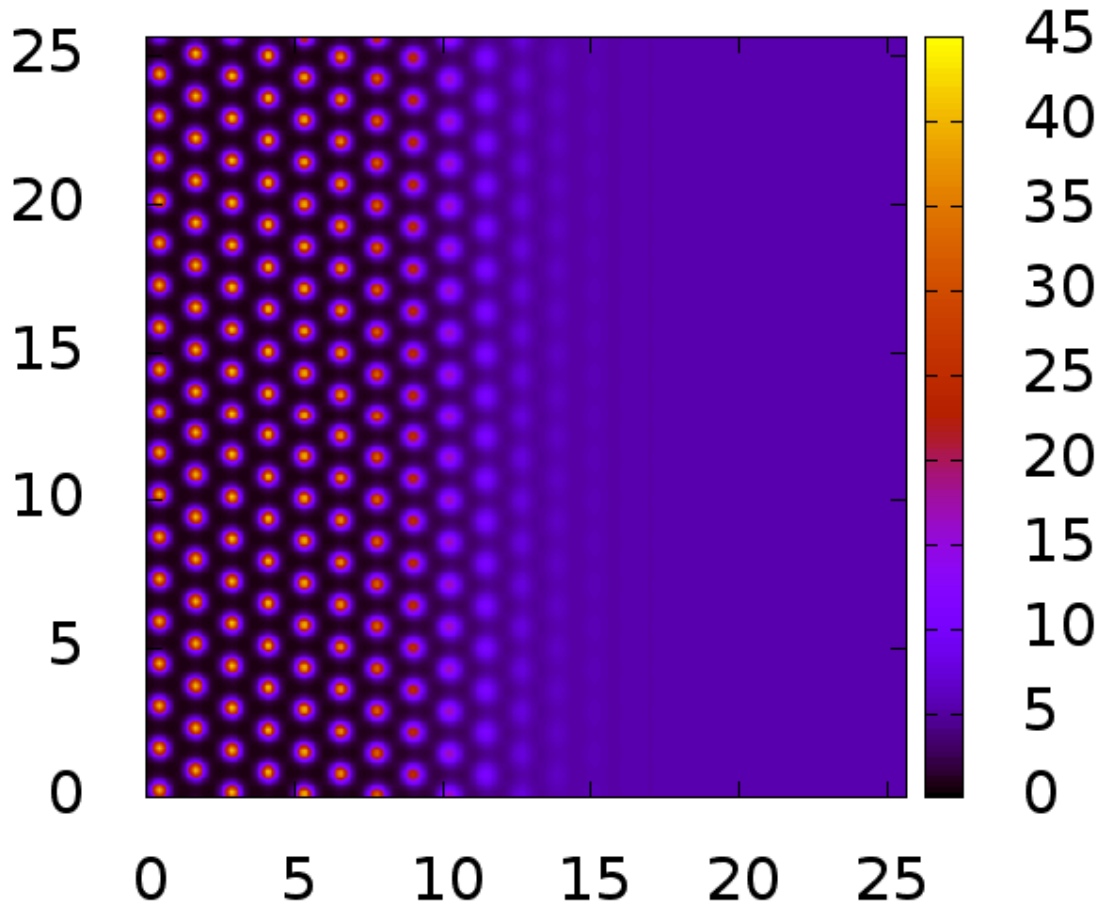

Density profile at the free interface between the coexisting liquid and solid phases in a GEM-4 model liquid ($v(r) = \epsilon \exp -(r/R)^4$) when $\mu = 17 k_B T$, $k_B T = 1$.

The Phase Field Crystal model

In one dimension, with $\alpha = 1$ and $q = 1$, we have

$$\partial_t \phi = \partial_x^2 \left[r\phi + (1 + \partial_x^2)^2 \phi + \phi^3 \right].$$

This equation is reversible in space (i.e., it is invariant under $x \to -x$).
Moreover, it conserves the total "mass" $\phi_0 \equiv L^{-1} \int_0^L \phi \, dx$, where L is the size of the system.
Linearizing about $\phi = \phi_0$ results in the dispersion relation

$$\sigma = -k^2 \left[r + (1 - k^2)^2 + 3\phi_0^2 \right],$$

and hence instability for $r < -3\phi_0^2$:

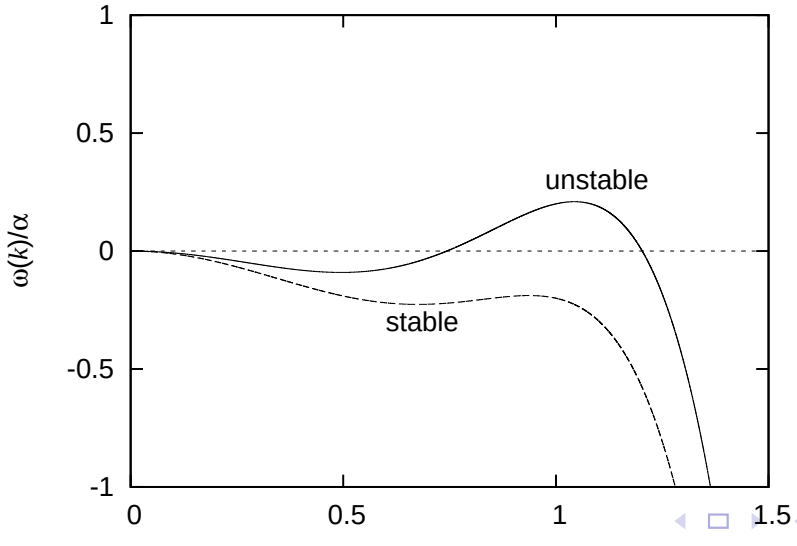

Crystallization front at $r = -0.9$, $\phi_0 = -0.43$

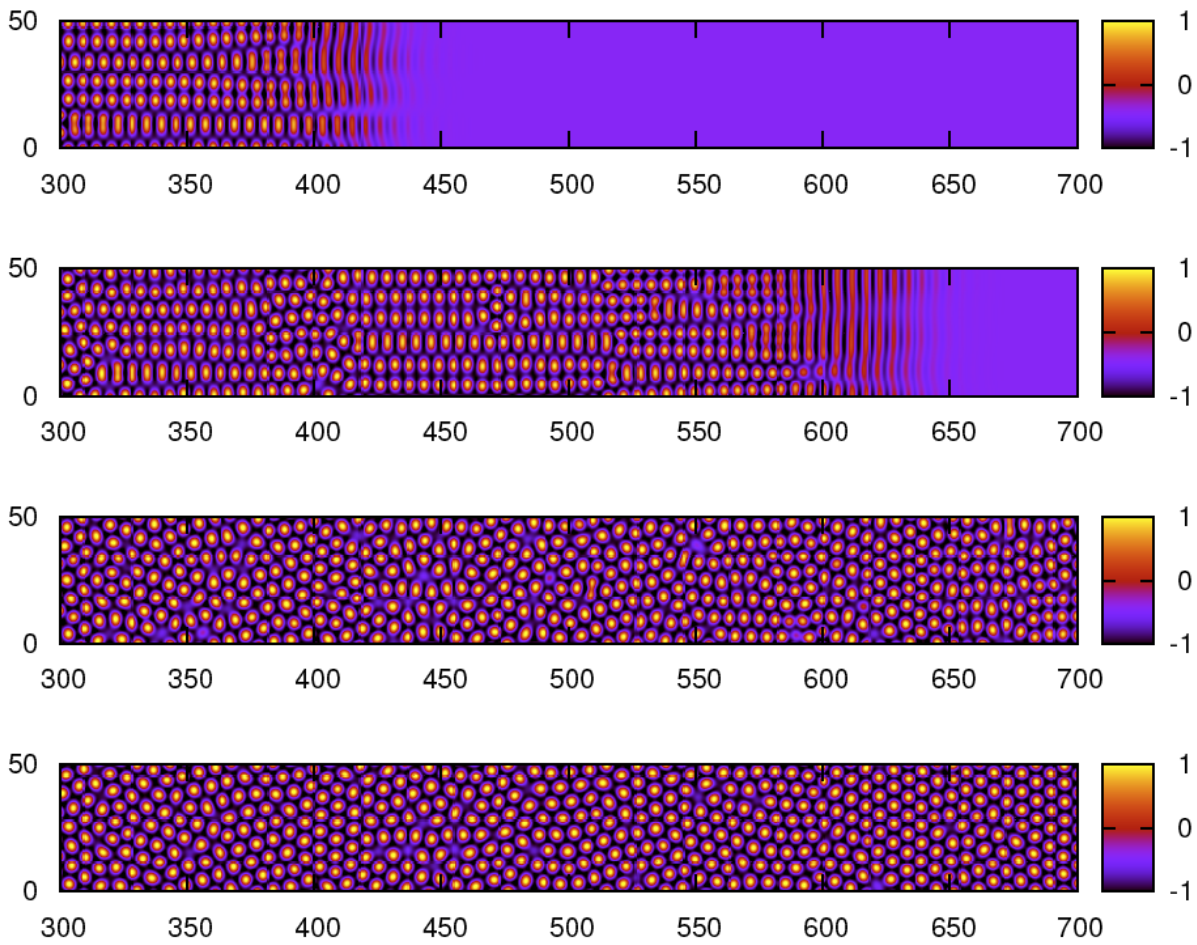

Archer et al., PRE **86**, 031603 (2012)

Crystallization fronts: parameter dependence

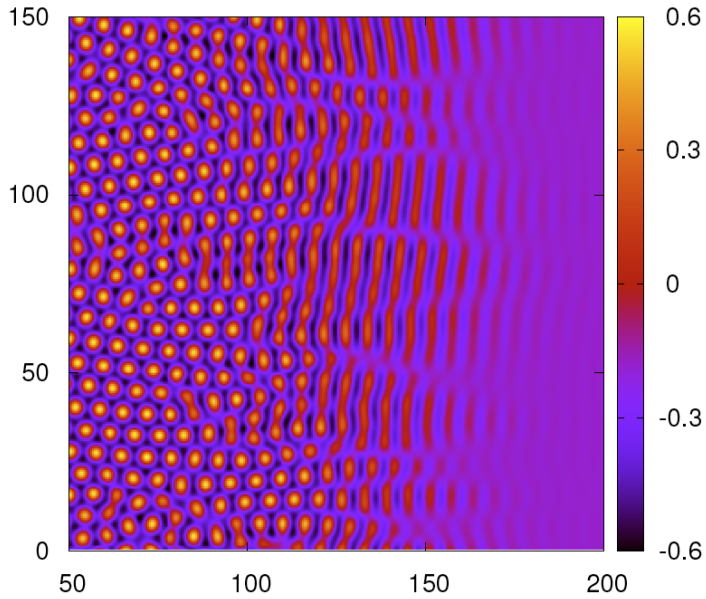

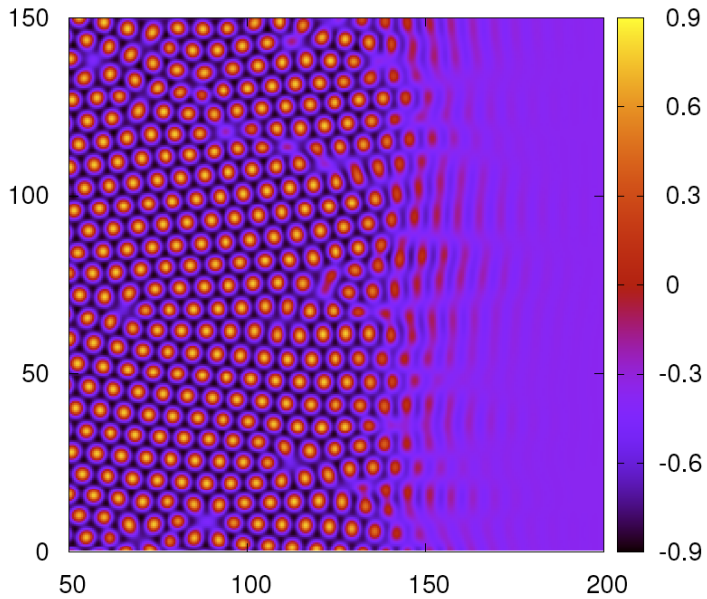

$r = -0.2$, $\phi_0 = -0.183$ $\quad$ $r = -0.5$, $\phi_0 = -0.365$

Archer et al., PRE **86**, 031603 (2012)

Bond angle and radial correlation function for $r = -0.9$

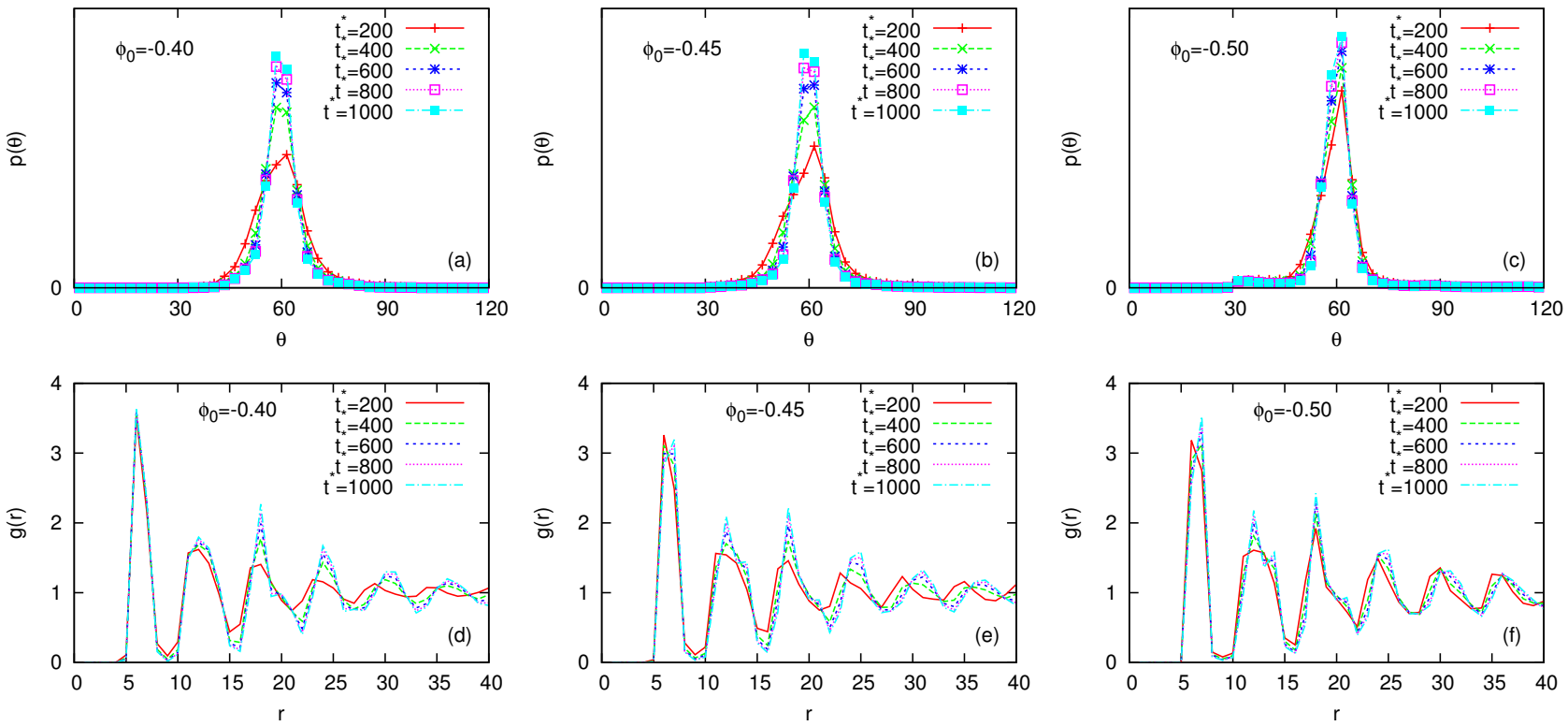

Archer et al., PRE **86**, 031603 (2012)

1D crystallization front: $r = -0.9$, $\phi_0 = -0.4$

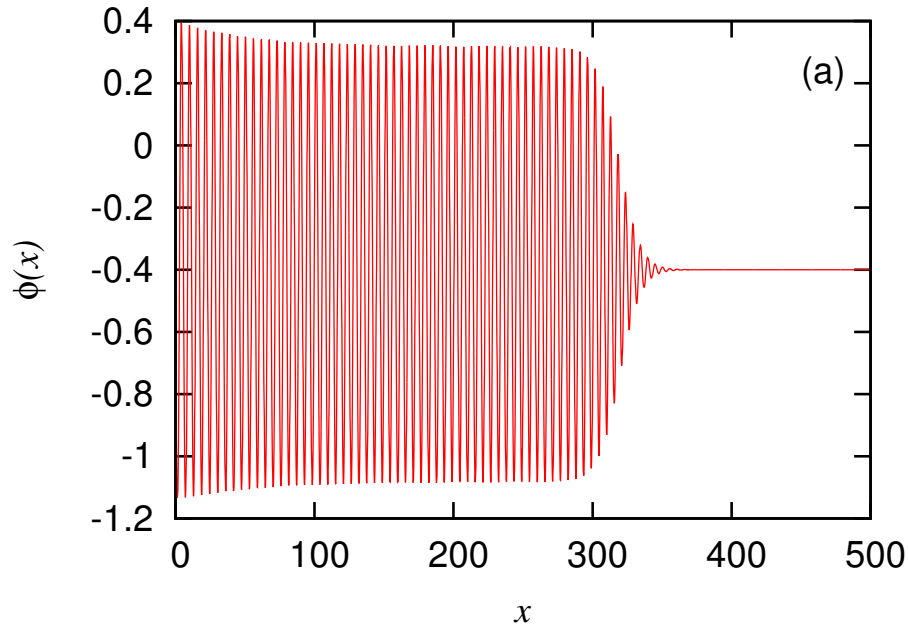

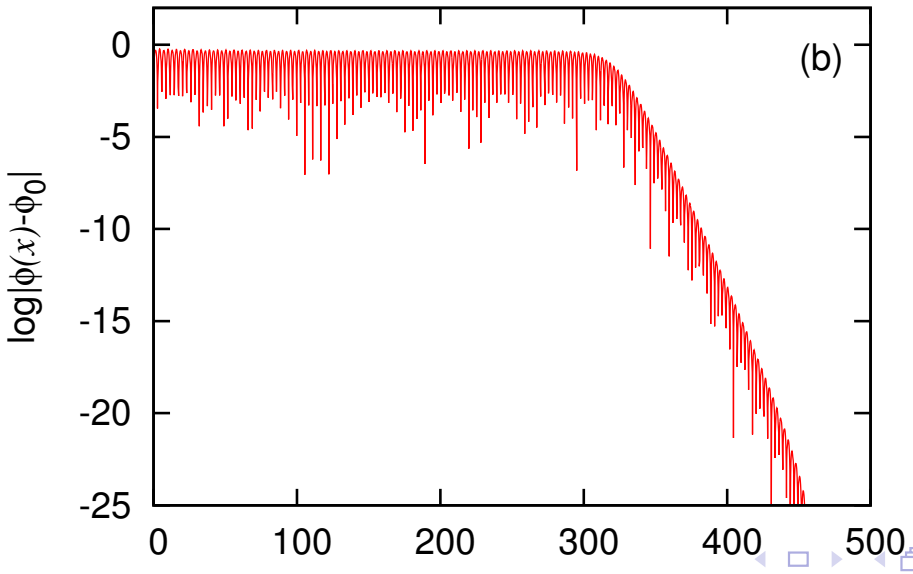

Speed of the crystallization front

We assume that the speed of the front is determined by the marginal stability criterion of Dee and Langer, and write the linearized equation in the form

$$\sigma(k) = -\alpha k^2[\Delta + (q^2 - k^2)^2],$$

where $\Delta = r + 3\phi_0^2 < 0$. To determine the front speed we go into the frame of the front moving at speed c, $\omega(k) = ick + \sigma(k)$, and solve

$$\frac{d\omega}{dk} = 0, \qquad \mathrm{Re}(\omega) = 0$$

for k_r, k_i and c as functions of Δ. The resulting density profile at the front is $\tilde{\rho}_{\mathrm{front}}(\xi, t) \sim \exp(-k_i\xi)\sin(k_r\xi + \mathrm{Im}(\omega)t)$ relative to the front. The pattern left behind is periodic in space with wavenumber k^* given by conservation of nodes [Ben-Jacob et al, Physica D **14**, 348 (1985)]

$$k^* = \frac{1}{c}\mathrm{Im}(\omega) = k_r + \frac{1}{c}\mathrm{Im}[\sigma(k)].$$

[see also Galenko and Elder, Phys. Rev. B **83**, 064113 (2011)]

Speed of the crystallization front in 1D

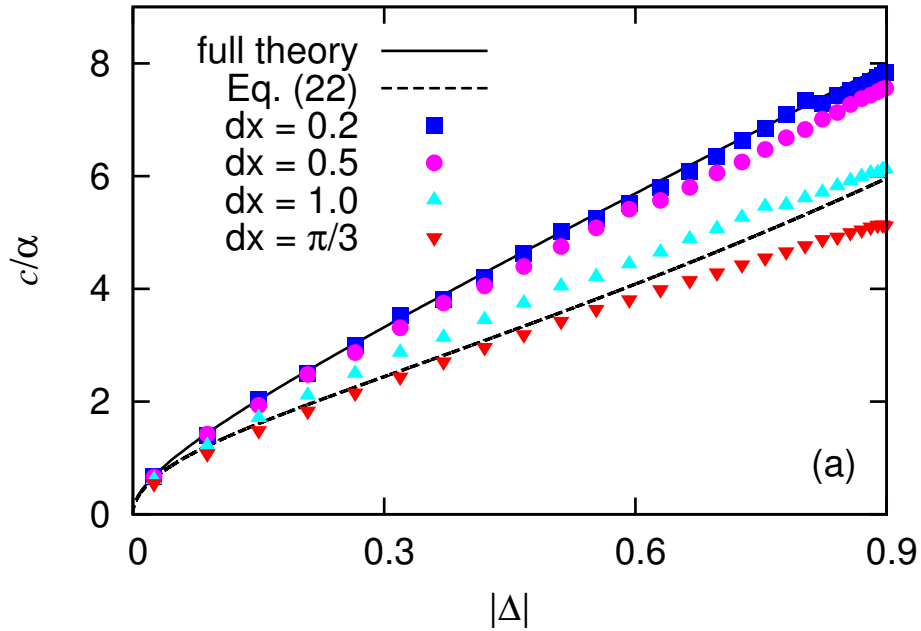

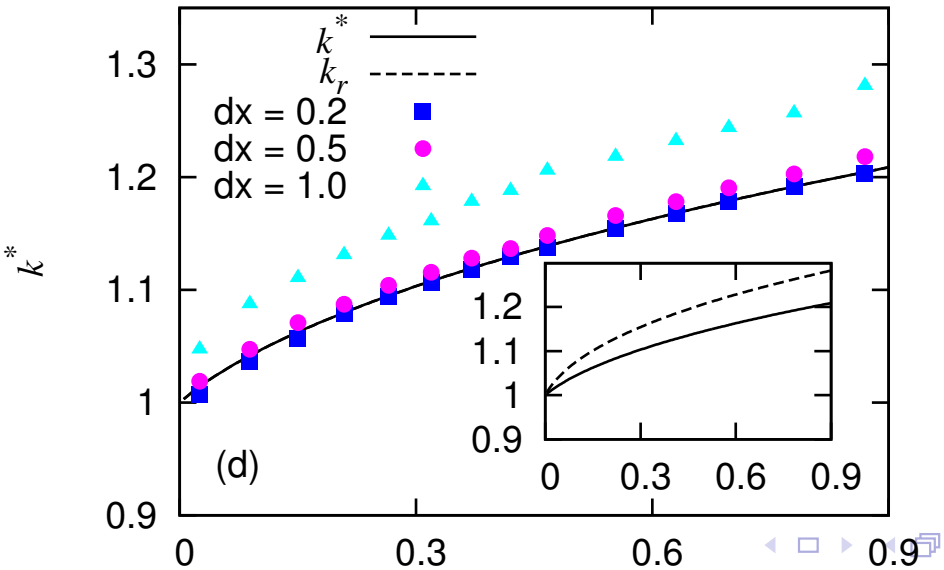

Crystallization front in 2D: 1-component GEM-4

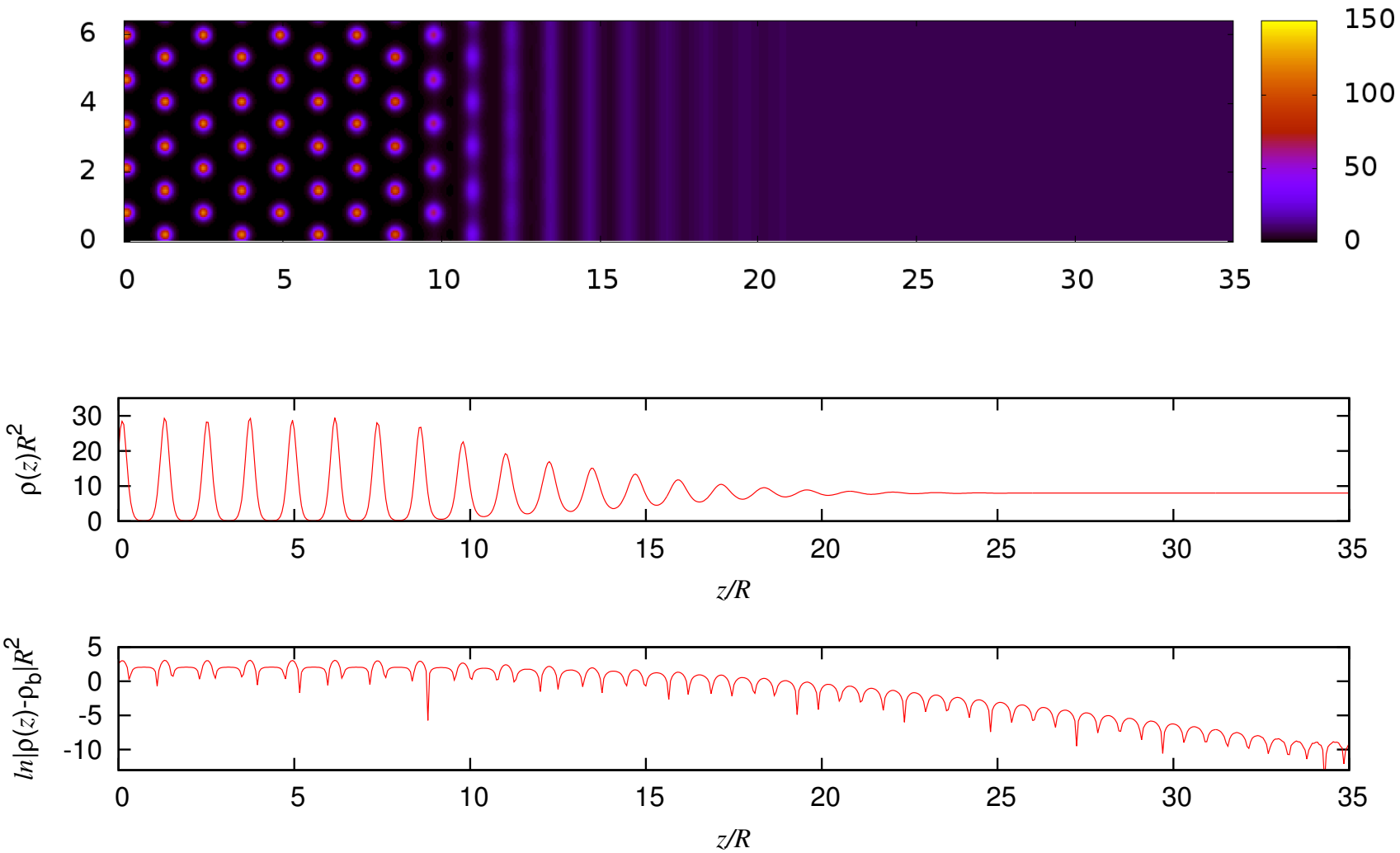

Density profile for a crystallization front advancing from left to right into the unstable GEM-4 liquid with bulk density $\rho_0 R^2 = 8$ and temperature $\epsilon = k_B T$,

Speed of crystallization front in 2D: 1-component GEM-4

The 2D case is much more complicated but also more interesting because of the competition between stripes (first pattern to form) and hexagons (final pattern to form):

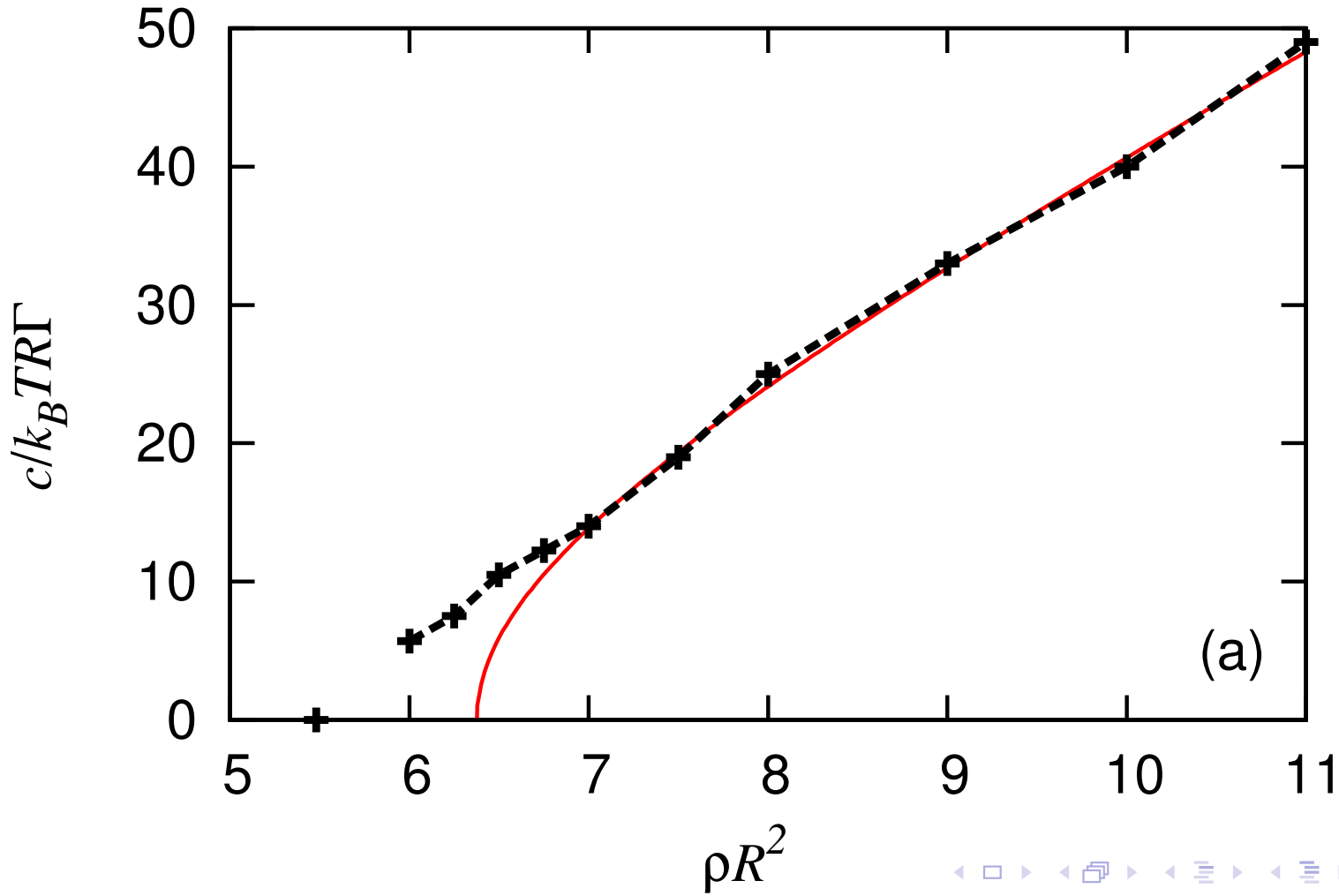

Speed of the crystallization front in 2D

Model equations:

$$\frac{\partial A_k}{\partial t} = \gamma A_k + \frac{\partial^2 A_k}{\partial x_k^2} + A^*_{[k-1]} A^*_{[k+1]} - (|A_k|^2 + \lambda |A_{[k-1]}|^2 + \lambda |A_{[k+1]}|^2) A_k,$$

where $k = 0, 1, 2$. Here A_k are the complex amplitudes of the three wavevectors $\mathbf{n}_0 \equiv (1, 0)q$, $\mathbf{n}_1 \equiv (-1, \sqrt{3})q/2$, $\mathbf{n}_2 \equiv (-1, -\sqrt{3})q/2$ in the (x, y) plane, and $x_k \equiv \mathbf{x} \cdot \mathbf{n}_k$ [Golubitsky et al., Phys. D **10** 249 (1984)]. Here q is the critical wavenumber at onset of the hexagon- forming instability ($\gamma = 0$), and $[k \pm 1] \equiv (k \pm 1)(\mathrm{mod} 3)$. These equations constitute a gradient flow with free energy

$$\mathcal{F} \equiv \int_{-\infty}^{\infty} dx \left(\sum_{k=0}^{2} \frac{1}{2} |\frac{\partial A_k}{\partial x_k}|^2 - V \right),$$

where

$$V \equiv \sum_{k=0}^{2} \left(\frac{1}{2} \gamma |A_k|^2 - \frac{1}{4} |A_k|^4 \right) - \frac{\lambda}{2} \left(|A_0|^2 |A_1|^2 + |A_1|^2 |A_2|^2 + |A_2|^2 |A_0|^2 \right) + A_0^* A_1^* A_2^*.$$

Speed of the crystallization front in 2D

We focus on planar fronts perpendicular to $\mathbf{n}_0 \equiv (1,0)q$ and thus focus on solutions independent of the variable y along the front. Symmetry with respect to $y \to -y$ implies the presence of solutions with $A_1 = A_2 \equiv B$, say. Absorbing the wavenumber q in the variable x and writing $A_0 \equiv A$ we obtain the equations

$$\frac{\partial A}{\partial t} = \frac{\partial^2 A}{\partial x^2} + \gamma A + B^2 - A^3 - 2\lambda A B^2$$

$$\frac{\partial B}{\partial t} = \frac{1}{4}\frac{\partial^2 B}{\partial x^2} + \gamma B + AB - (1+\lambda)B^3 - \lambda A^2 B.$$

In writing these equations we have assumed that A and B are real in order to focus on the behavior of the amplitudes, thereby setting the phase $\Phi \equiv \arg(A) + 2\arg(B) = 0$. This phase distinguishes the so-called up-hexagons from down-hexagons [Golubitsky et al., Phys. D **10**, 249 (1984)]. These equations form the basis for the theory that follows [Hari & Nepomnyashchyy, PRE **61**, 4835 (2000); Doelman et al., Euro. J. Appl. Math. **14**, 85 (2003)].

Speed of the crystallization front in 2D

These equations have solutions in the form of regular hexagons $(A, B) = (A_h, A_h)$, stripes $(A, B) = (A_s, 0)$ and the homogeneous liquid state $(A, B) = (0, 0)$, where without loss of generality

$$A_h = \frac{1 + \sqrt{1 + 4\gamma(1 + 2\lambda)}}{2(1 + 2\lambda)}, \qquad A_s = \sqrt{\gamma};$$

these are critical points of the potential

$$V(A, B) \equiv \frac{1}{2}\gamma(A^2 + 2B^2) + AB^2 - [\frac{1}{4}A^4 + \lambda A^2 B + \frac{1}{2}(1 + \lambda)B^4].$$

The hexagons and the liquid state coexist stably in the subcritical regime, $\gamma_{sn} < \gamma < 0$, where $\gamma_{sn} = -[4(1 + 2\lambda)]^{-1}$. For $\gamma > 0$ the liquid state becomes unstable, creating a branch of unstable stripes; stable hexagons continue to exist.

The potential $V(A, B)$

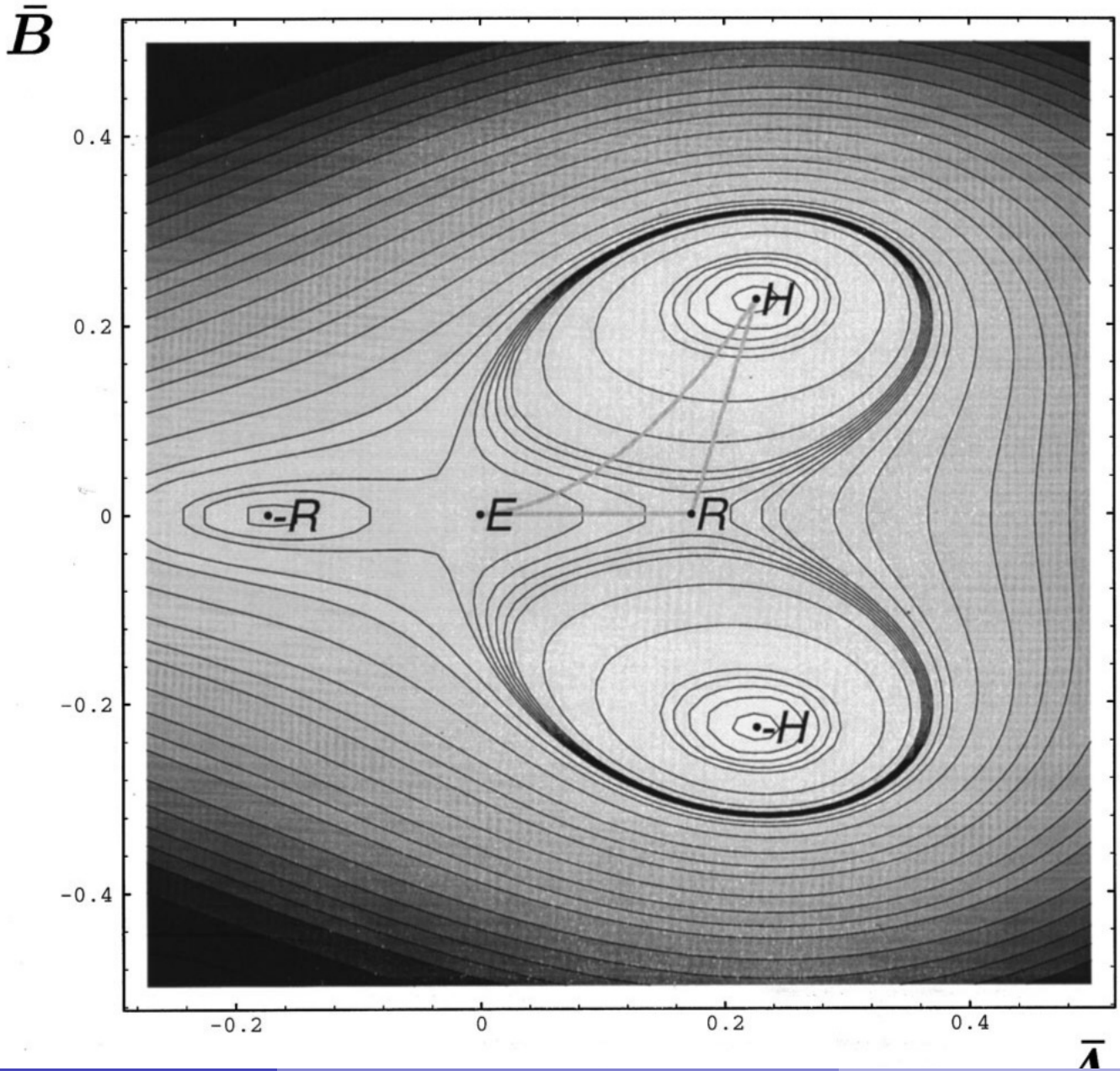

Speed of the crystallization front in 2D

A front traveling with speed c to the right, connecting the hexagonal state on the left with the liquid state to the right, takes the form

$$A(x,t) = \tilde{A}(\xi), \quad B(x,t) = \tilde{B}(\xi), \quad \xi \equiv x - ct.$$

Thus

$$\frac{\partial^2 \tilde{A}}{\partial \xi^2} + c\frac{\partial \tilde{A}}{\partial \xi} + \gamma \tilde{A} + \tilde{B}^2 - \tilde{A}^3 - 2\lambda \tilde{A}\tilde{B}^2 = 0,$$

$$\frac{1}{4}\frac{\partial^2 \tilde{B}}{\partial \xi^2} + c\frac{\partial \tilde{B}}{\partial \xi} + \gamma \tilde{B} + \tilde{A}\tilde{B} - (1+\lambda)\tilde{B}^3 - \lambda \tilde{A}^2 \tilde{B} = 0$$

with the boundary conditions

$$\tilde{A} = \tilde{B} = A_h \quad \text{as} \quad \xi \to -\infty, \qquad \tilde{A} = \tilde{B} = 0 \quad \text{as} \quad \xi \to \infty.$$

The speed c vanishes in the subcritical regime when $\gamma = \gamma_M < 0$ defined by the requirement $V(A_h, A_h) = V(0,0) = 0$ and is positive for $\gamma > \gamma_M$ ($V(A_h, A_h) < 0$) and negative for $\gamma < \gamma_M$ ($V(A_h, A_h) > 0$).

An elementary calculation gives $\gamma_M = -2[9(1+2\lambda)]^{-1} < 0$ (Maxwell).

Energetics: Maxwell point

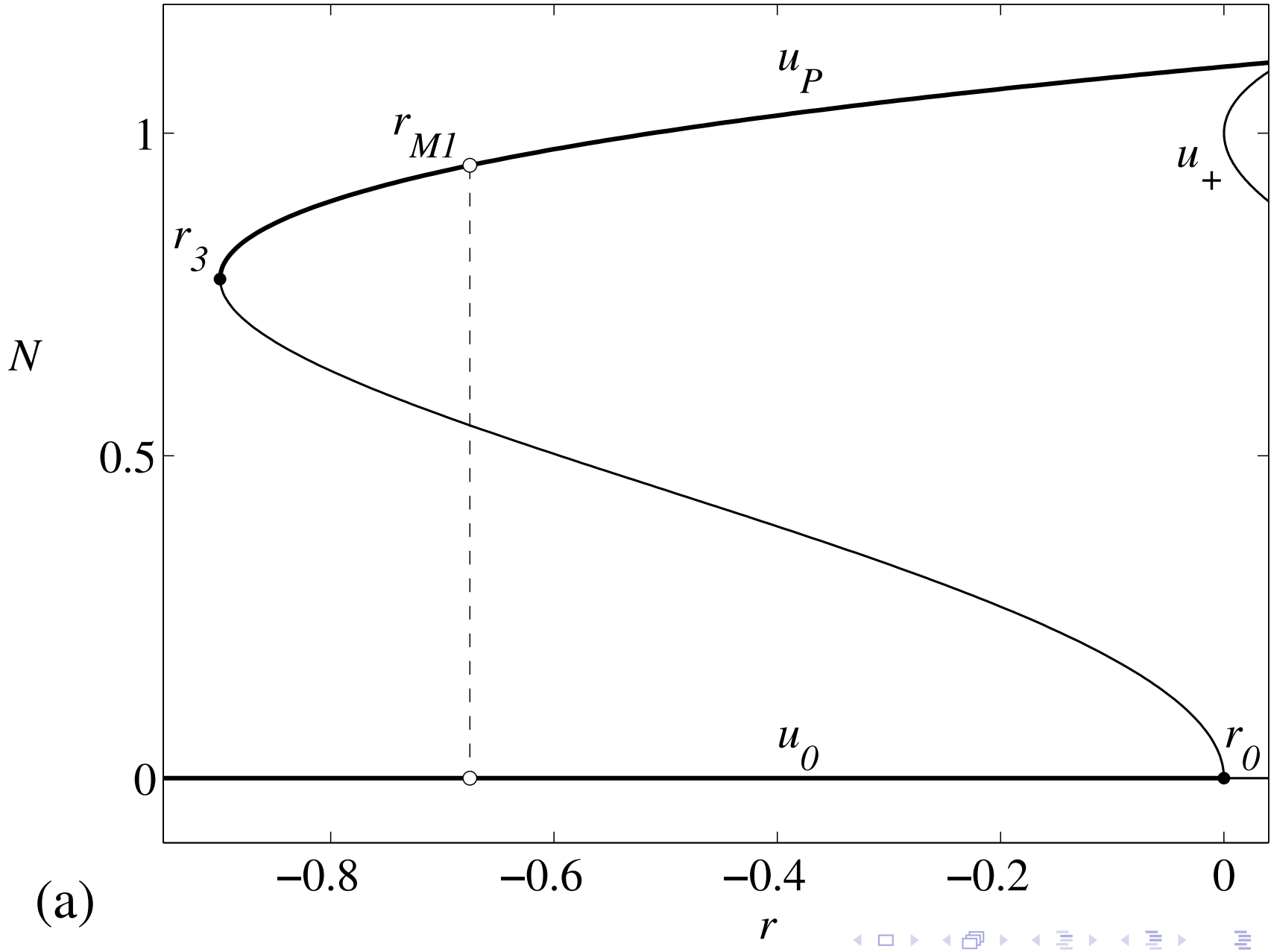

Speed of the crystallization front in 2D

The situation is more complicated in the supercritical regime where $\gamma > 0$ because this regime contains supercritical (but unstable!) stripes oriented parallel to the front. As a result one now finds fronts that connect the hexagonal structure to the stripe pattern and the stripe pattern to the liquid state, in addition to the front connecting the hexagonal structure and the (unstable) liquid state.

The marginal stability condition implies that stripes invade the homogeneous state with speed $c_s = 2\sqrt{\gamma}$, while an analogous calculation shows that the hexagons invade the unstable stripes with speed $c_{hs} = [\sqrt{\gamma} - (\lambda - 1)\gamma]^{1/2}$. This speed exceeds the speed c_s in the interval $0 < \gamma < (\lambda + 3)^{-2}$.

It is evident that the speed c_s cannot be selected when γ is too close to threshold since the front speed c_h remains positive for all $\gamma > \gamma_M$ ($\gamma_M < 0$).

Speed of a crystallization front in 2D: model problem

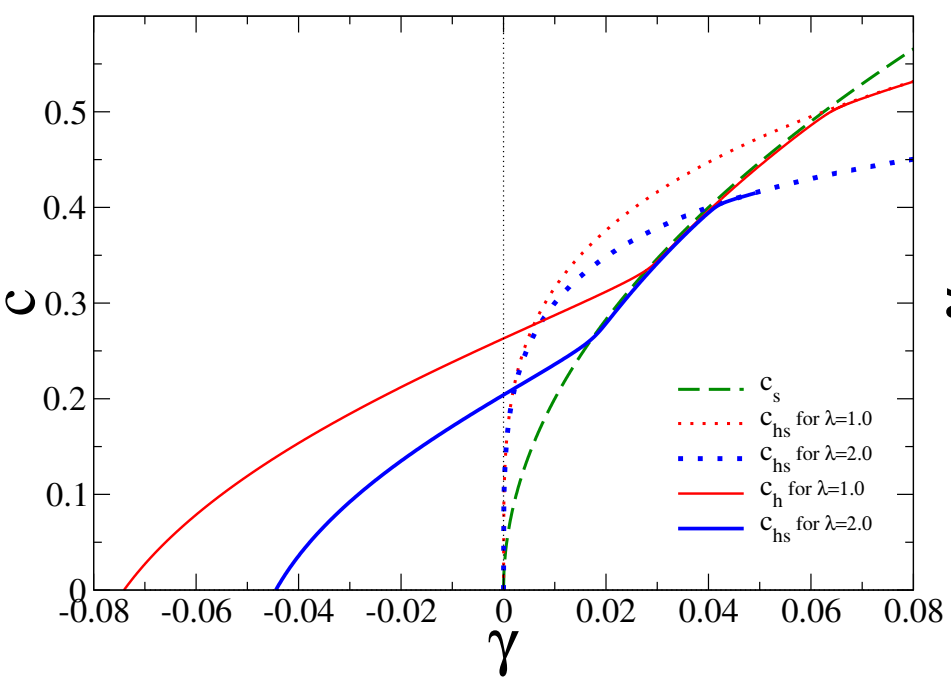

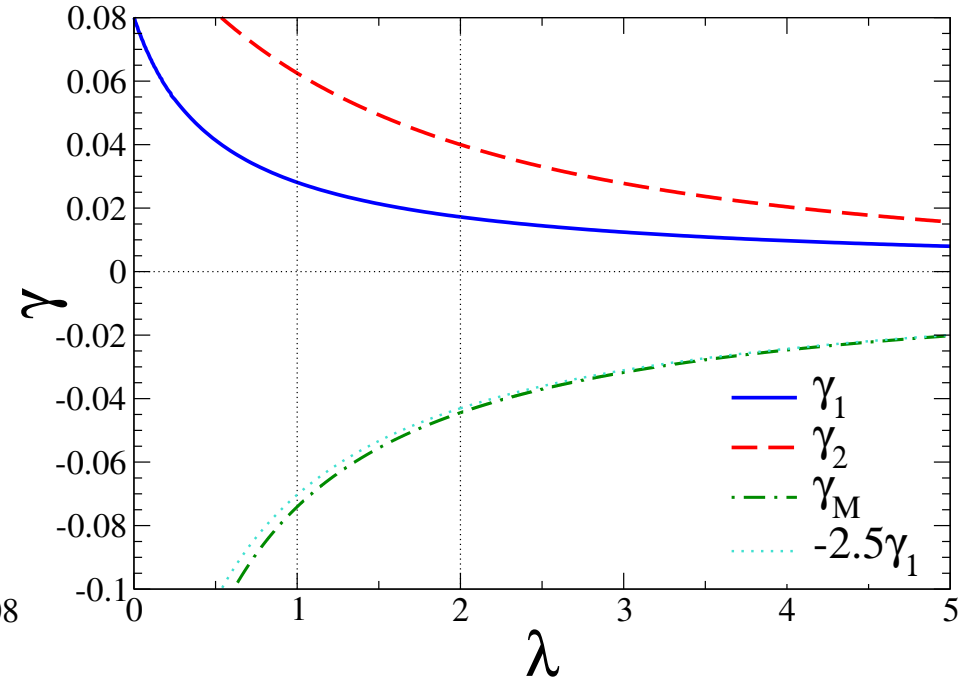

The point $\gamma = \gamma_1$ is the point of intersection of c_h and c_s and corresponds to an **orbit flip**. The point $\gamma = \gamma_2$ is the point $c_{hs} = c_s$. The model predicts that $\gamma_M \approx -2.5\gamma_1$ for all λ, a result that is not in agreement with the GEM-8 simulation. This may be because of (i) absence of **pinning** in the model equations, (ii) omission of the $k = 0$ **mass mode**.

Quasicrystals

To generate quasicrystals we need an interaction between two spatial scales, with wavenumbers $q = q_s$ and $q = q_\ell$. Such an interaction occurs, for example, with the modified GEM-8 potential

$$V(r) = \epsilon e^{-(r/R)^8} + \epsilon a e^{-(r/R_s)^8}.$$

We pick $\beta\epsilon = 1$ and $R_s/R = 1.855$ so that $q_s/q_\ell \approx 2\cos(\pi/12) = 1.93$. We refer to the large scale ($q = q_\ell$) crystal as crystal A and the small scale ($q = q_s$) crystal as crystal B, and focus on the transition between these two periodic structures.

In two dimensions we solve the DFT equations and corroborate the results with Brownian dynamics simulations. We also perform DDFT simulations. In three dimensions there are many more competing structures and such calculations are more costly. We therefore employ the simpler PFC approach.

Quasicrystals in two dimensions

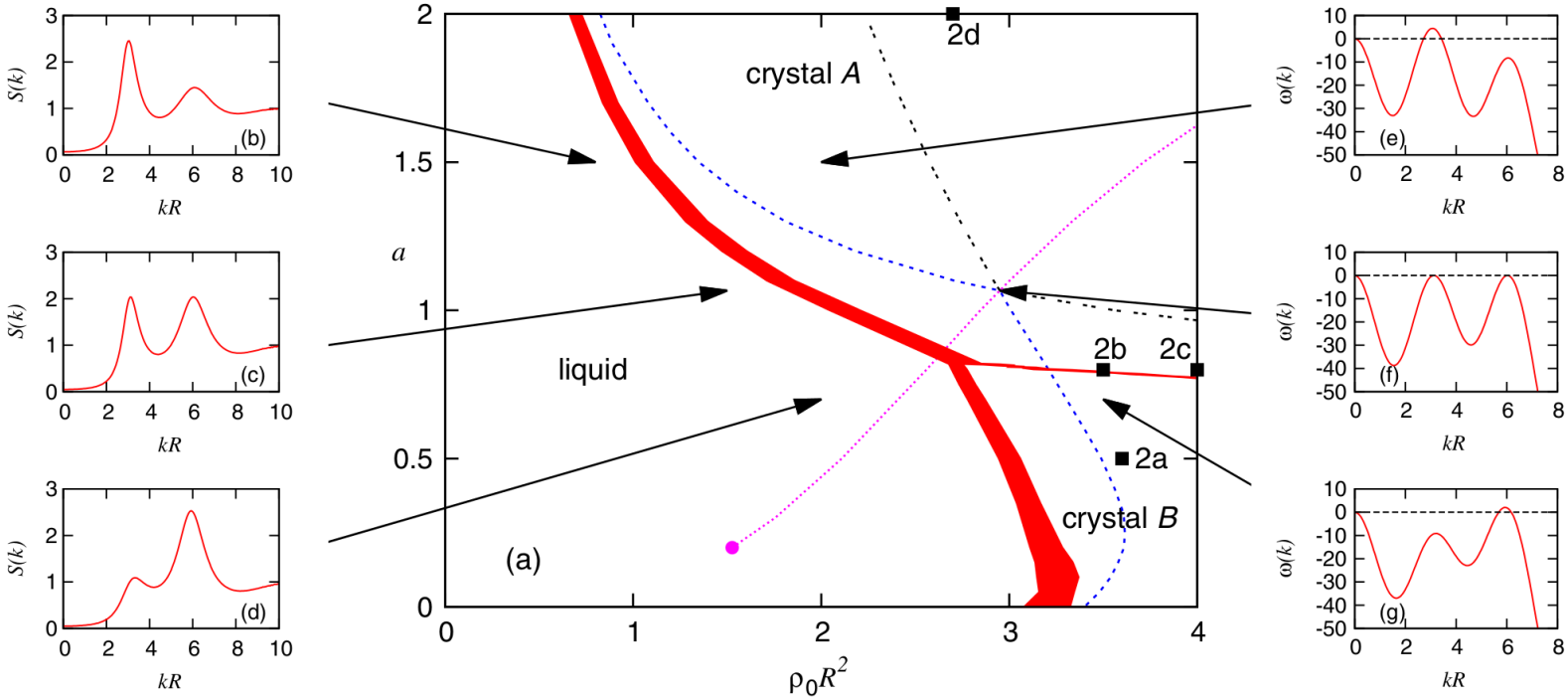

Phase diagram for the two-scale GEM-8 potential $V(r) = \epsilon e^{-(r/R)^8} + \epsilon a e^{-(r/R_s)^8}$ in two dimensions, with $\beta\epsilon = 1$ and $R_s/R = 1.855$.

Quasicrystals in two dimensions

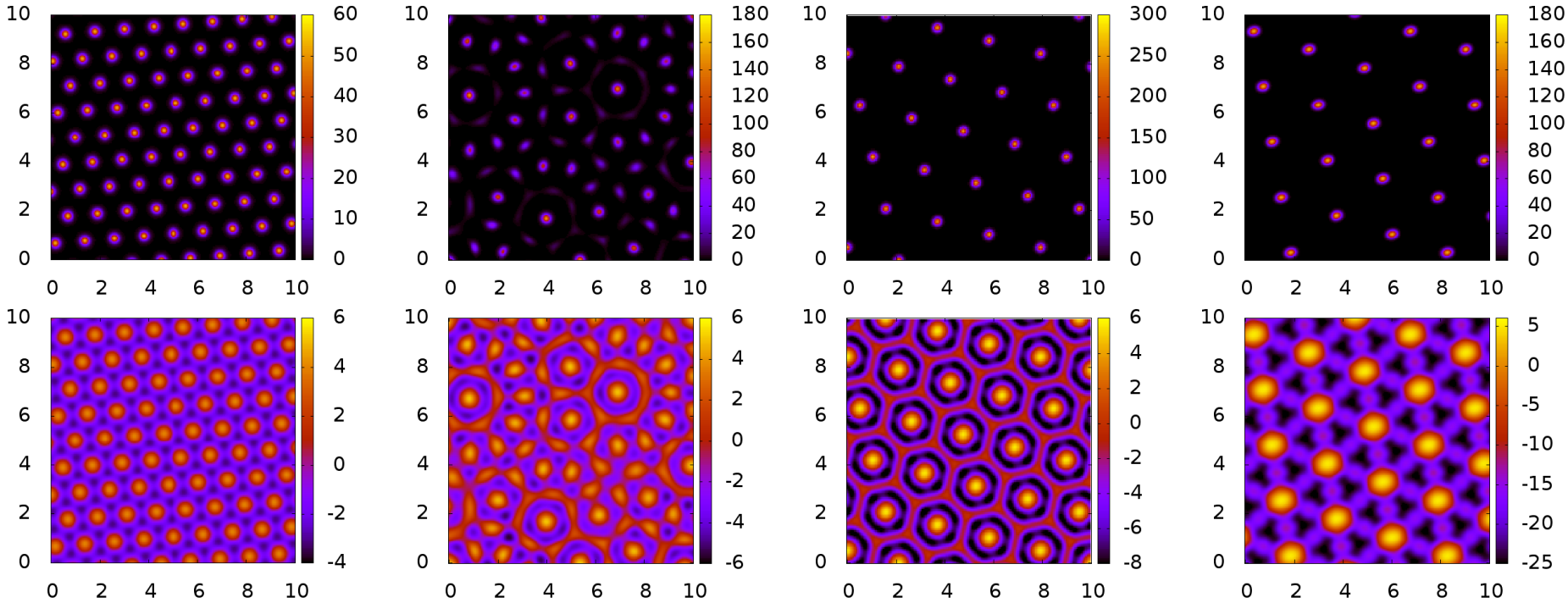

Density profiles at (a) $(\rho_0 R^2, a) = (3.6, 0.5)$ (typical of the small length scale crystal B), (b) $(3.5, 0.76)$, (c) $(4.0, 0.8)$ (both near the transition from crystal A to crystal B) and (d) $(2.7, 2)$ (typical of the large length scale crystal A). Top: $\rho(\mathbf{r})R^2$; bottom: $\ln[\rho(\mathbf{r})R^2]$

Quasicrystals in two dimensions

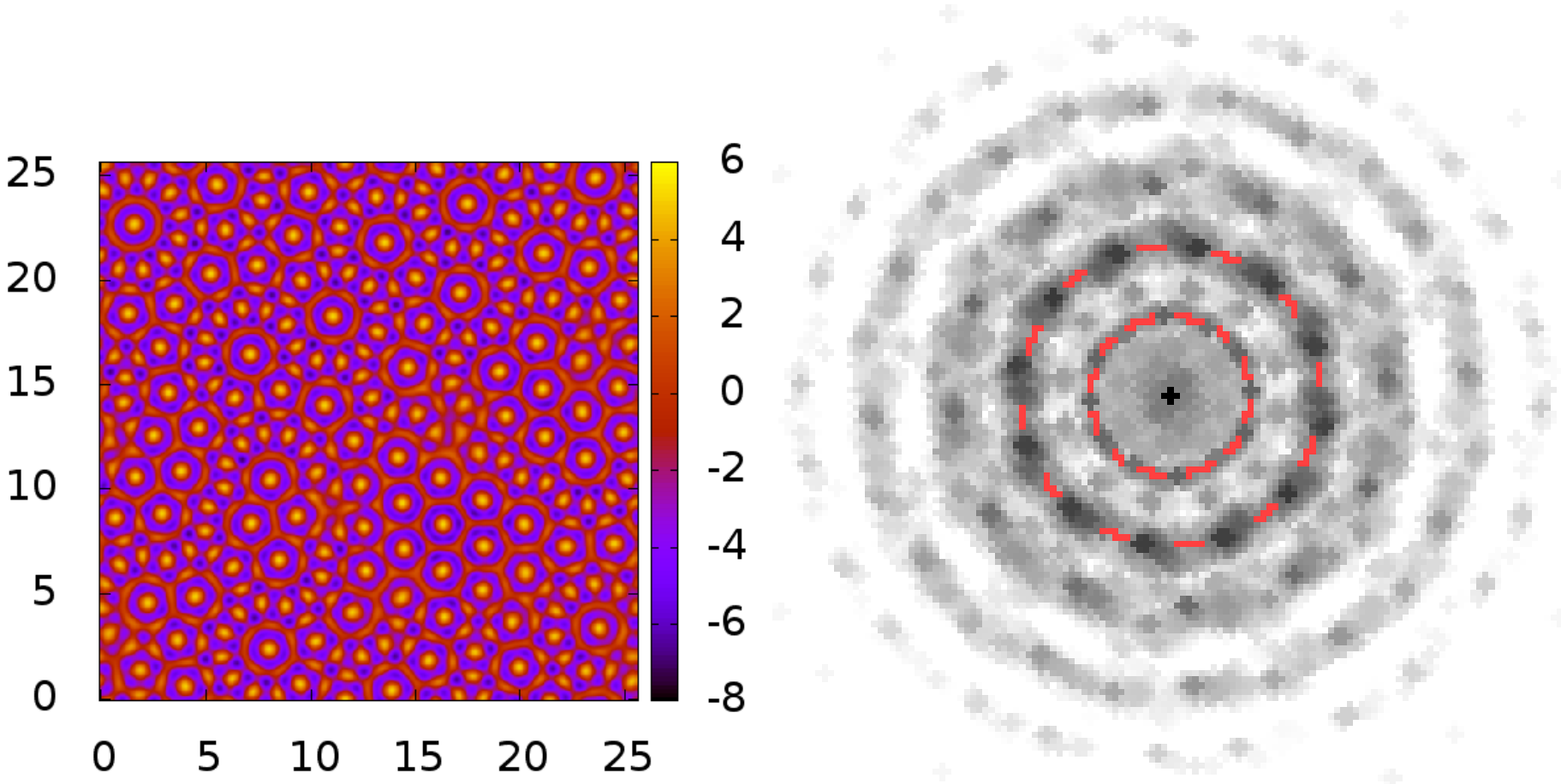

2D quasicrystal: (a) $\ln[\rho(r)R^2]$ in the $(x/R, y/R)$ plane obtained from DFT for $(\rho_0 R^2, a) = (3.5, 0.8)$ with random initial conditions. (b) The corresponding Fourier transform. The latter exhibits 12-fold symmetry, which is indicative of QC ordering.

Quasicrystals in two dimensions

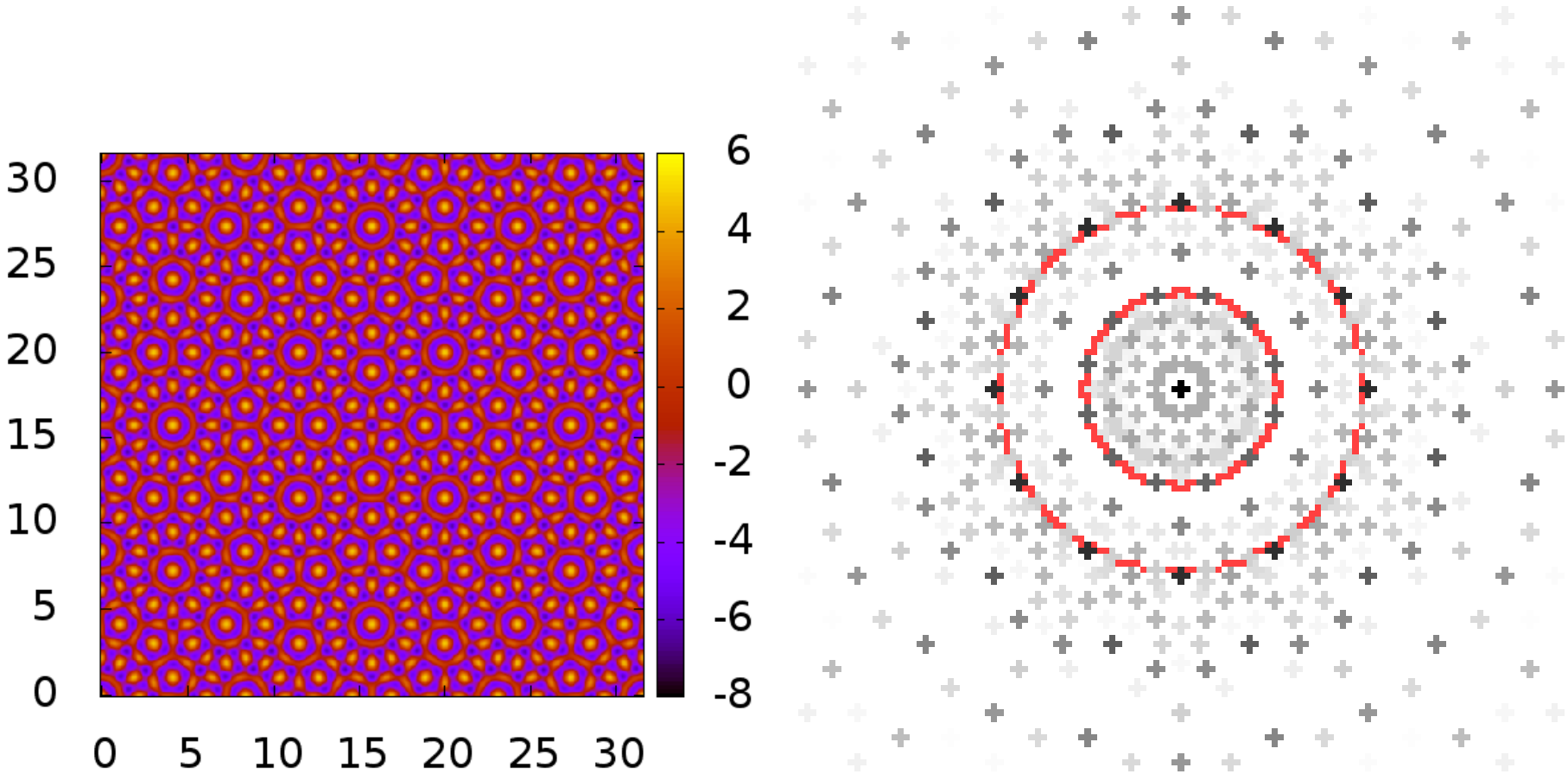

2D quasicrystal: (a) $\ln[\rho(r)R^2]$ in the $(x/R, y/R)$ plane obtained from DFT for $(\rho_0 R^2, a) = (3.5, 0.8)$ with initial conditions exhibiting QC ordering. (b) The corresponding Fourier transform.

Quasicrystals in 2D: Picard iteration

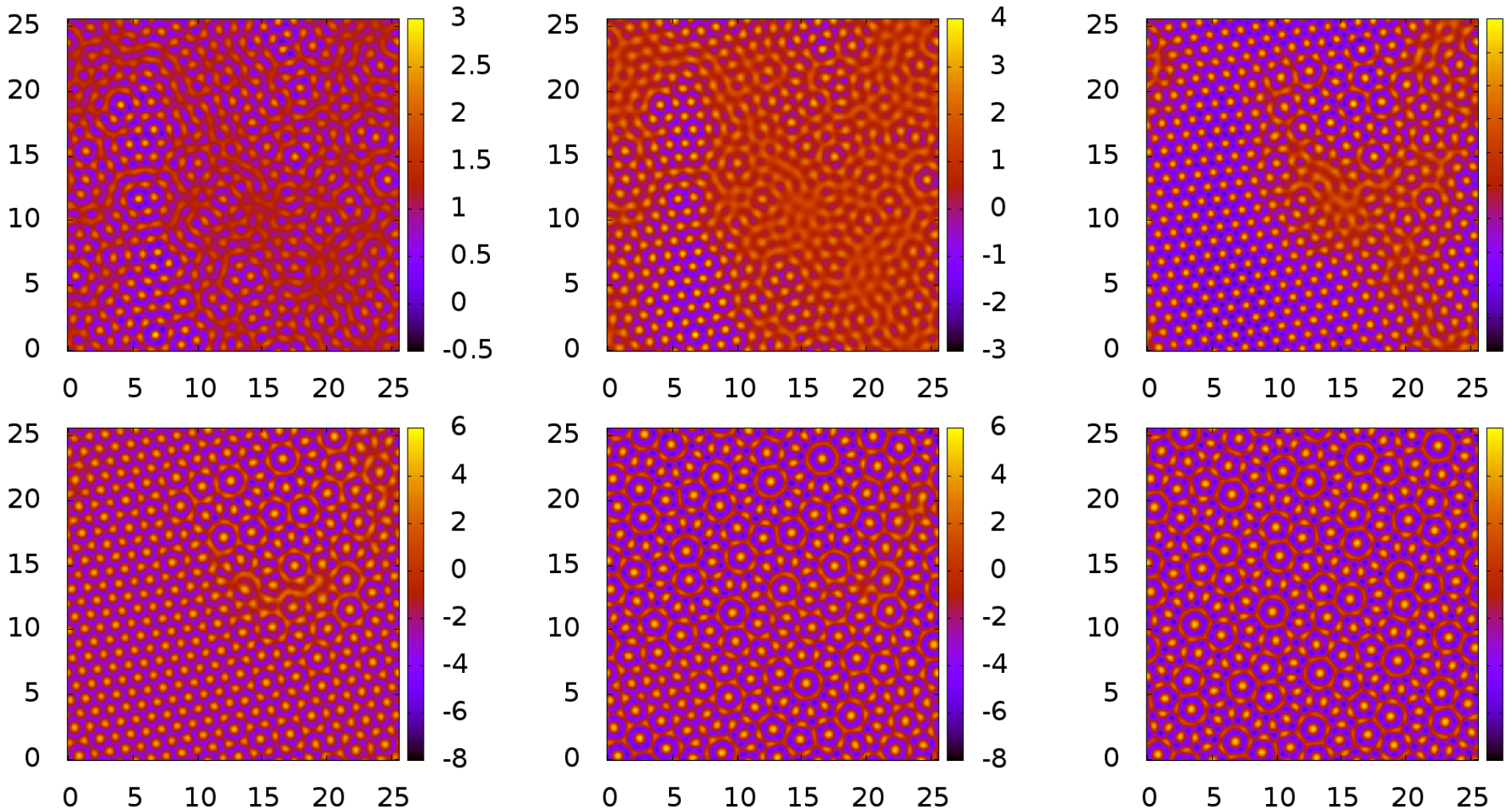

Figure: Time series of profiles $\ln[\rho(\mathbf{r})R^2]$ obtained via Picard iteration, for $a = 0.8$ and $\rho_0 R^2 = 3.5$, at $t = 30, 32, 35, 40, 50, 200$.

Quasicrystals in 2D: DDFT

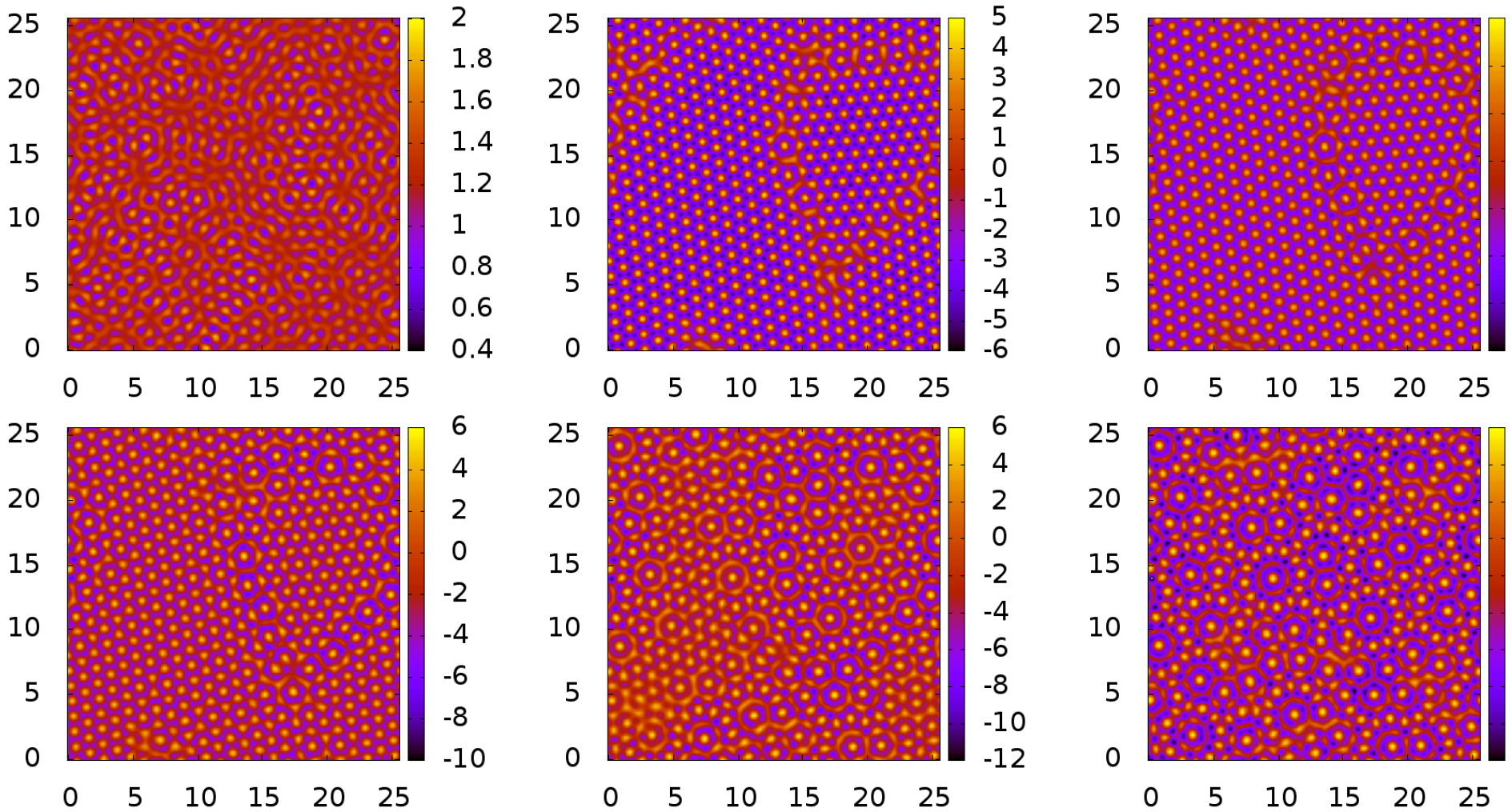

Figure: Time series of profiles $\ln[\rho(\mathbf{r})R^2]$ obtained from DDFT, for $a = 1.067$ and $\rho_0 R^2 = 3.5$, at $t^* = 1$, 2, 5, 10, 20 and 40.

Quasicrystals in two dimensions

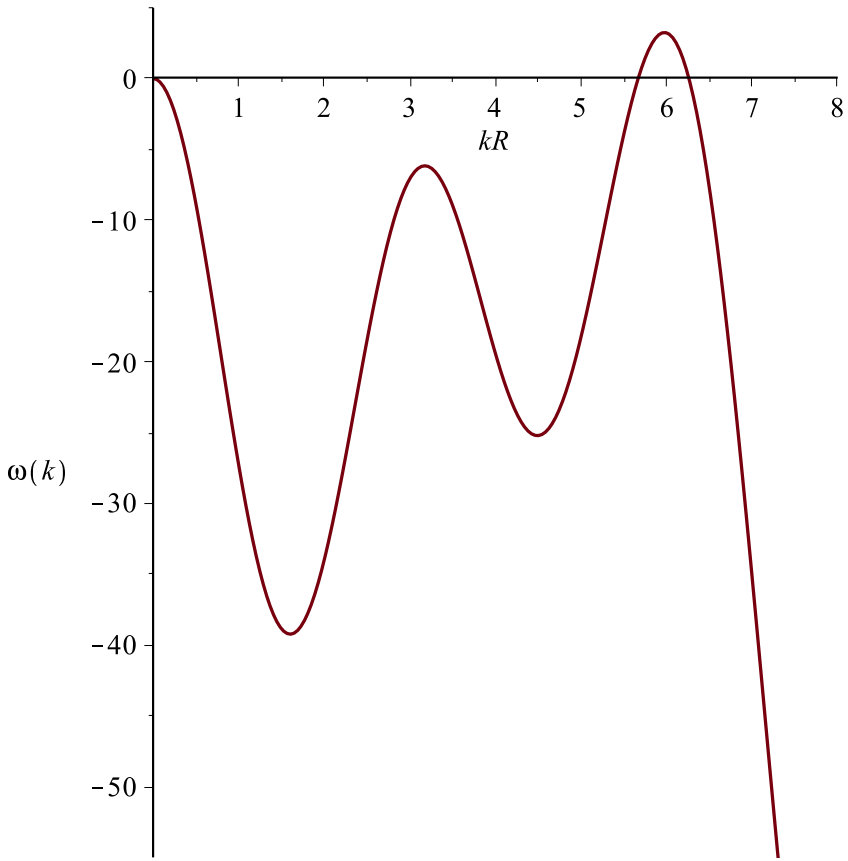

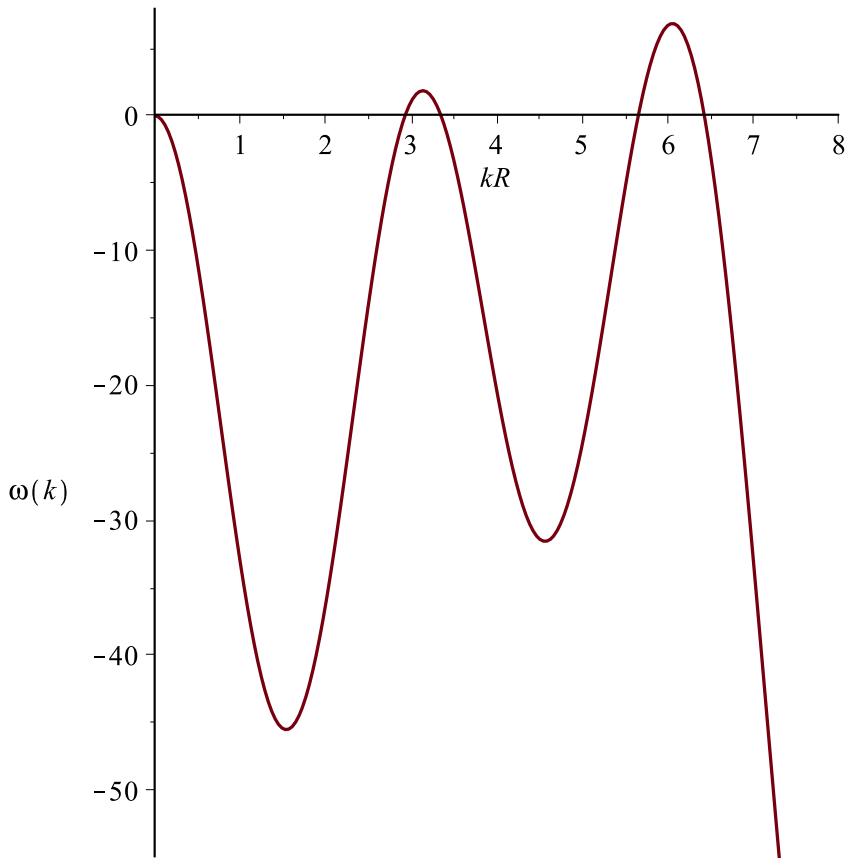

The dispersion relation at state point (a) $a = 0.8$, $\rho_0 R^2 = 3.5$ and (b) $a = 1.067$, $\rho_0 R^2 = 3.5$. QC form in either case: in (a) the large scale is triggered **nonlinearly**.

Quasicrystals in two dimensions

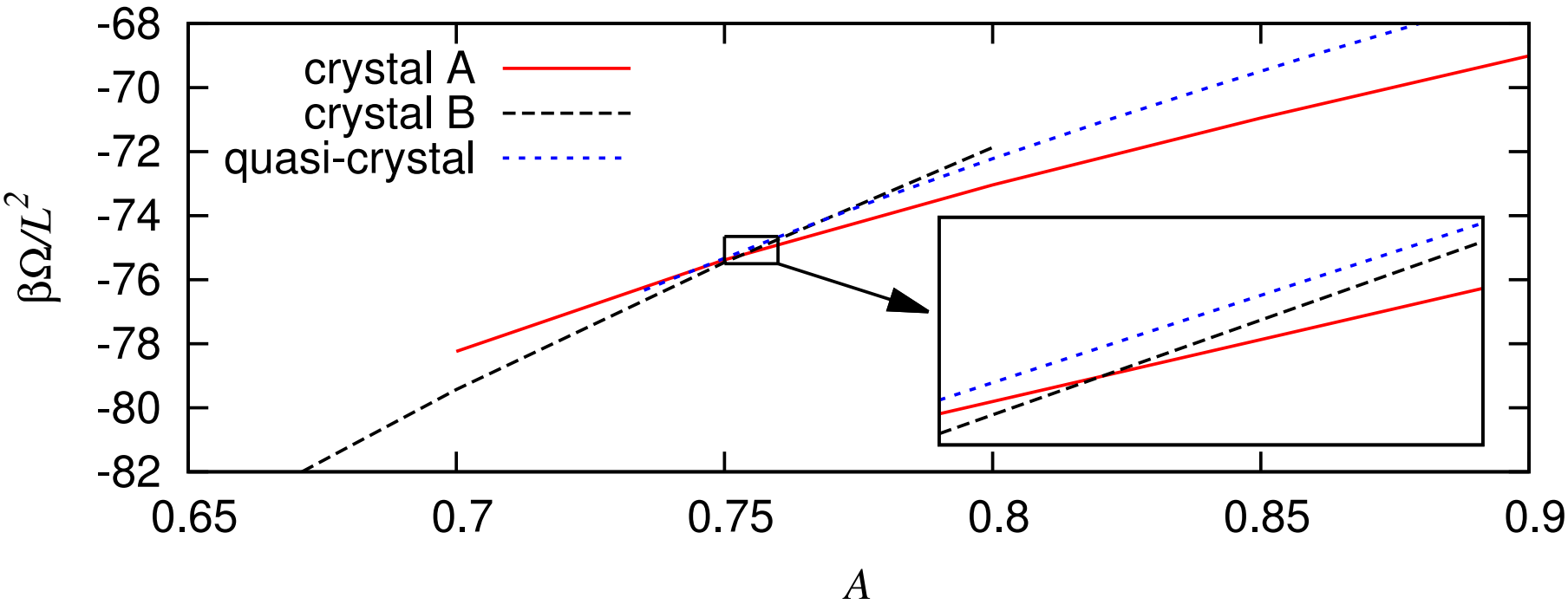

Grand potential density for $\beta\mu = 39$ as a function of the interaction parameter a

Quasicrystals in two dimensions

In this case we have two critical circles of radii q_s and $q_\ell < q_s$ and nonlinear three-wave interactions can occur between two waves on the inner circle and one on the outer, and vice versa. For the special case $q_s/q_\ell = 2\cos(\pi/12) \approx 1.93$ the angle between the two waves on the inner circle is 30° while the angle between the two waves on the outer circle is 150°. This wavelength ratio therefore allows 12 waves on each circle to interact through three-wave interactions and form a 12-fold QC, without the need to invoke additional waves. Any other length ratio potentially leads to an infinite number of interacting waves. This fact distinguishes 12-fold QC from all others, and may be the reason why 12-fold QC are commonly found in soft matter systems and Faraday waves.

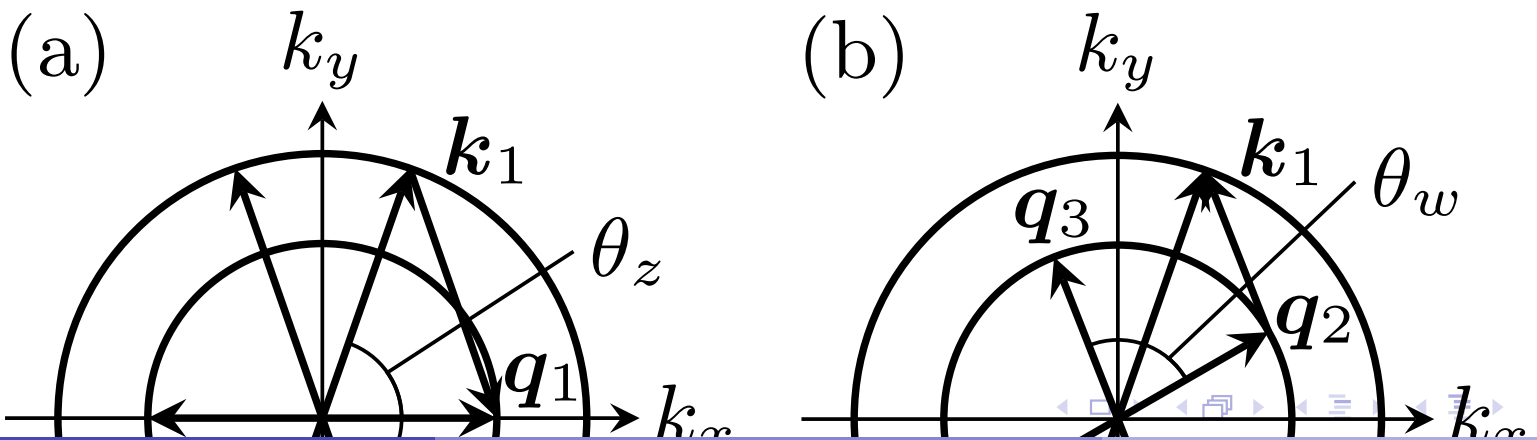

Quasipatterns in 2D: Ding and Umbanhowar, PRE (2006)

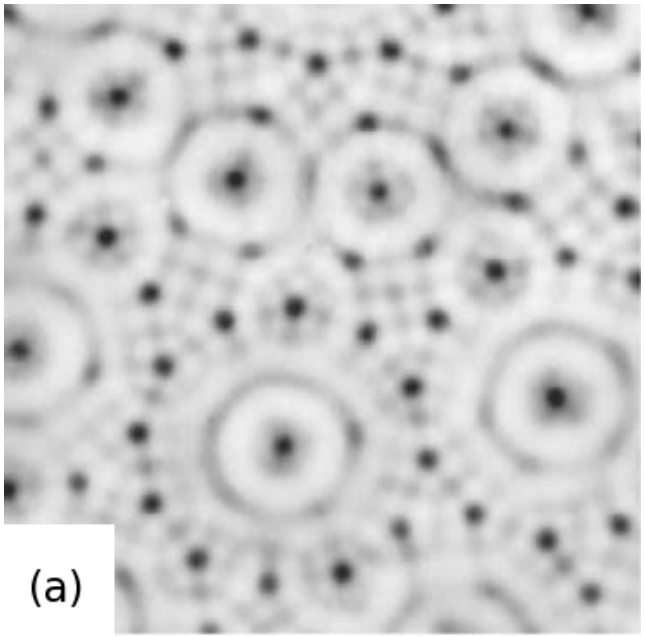

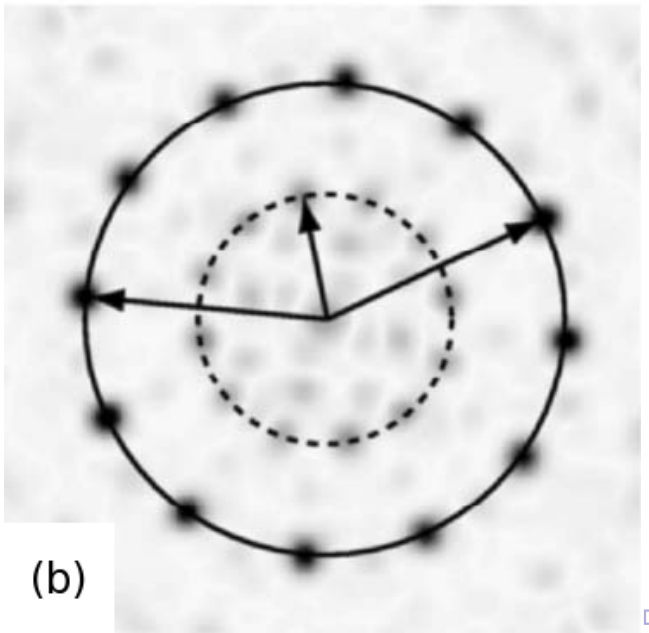

Quasicrystals in three dimensions

Our PFC model starts with a free energy $\mathcal{F}$:

$$\mathcal{F}[U] = \int \left[-\frac{1}{2} U \mathcal{L} U - \frac{Q}{3} U^3 + \frac{1}{4} U^4 \right] d\mathbf{x},$$

where the operator $\mathcal{L}$ and parameter Q are defined below. The evolution equation for U follows conserved dynamics and can be obtained from the free energy as

$$\frac{\partial U}{\partial t} = \nabla^2 \left(\frac{\delta \mathcal{F}[U]}{\delta U} \right) = -\nabla^2 \left(\mathcal{L} U + Q U^2 - U^3 \right).$$

We choose a linear operator $\mathcal{L}$ that allows marginal instability at two wavenumbers $k = 1$ and $k = q < 1$, with the growth rates of the two length scales determined by two independent parameters μ and ν. The resulting growth rate $\sigma(k)$ of a mode with wavenumber k is given by the polynomial $\sigma(k) = \frac{k^4[\mu A(k) + \nu B(k)]}{q^4(1-q^2)^3} + \frac{\sigma_0 k^2}{q^4}(1-k^2)^2 (q^2-k^2)^2$, where $A(k) = [k^2(q^2-3) - 2q^2 + 4](q^2-k^2)^2 q^4$ and $B(k) = [k^2(3q^2-1) + 2q^2 - 4q^4](1-k^2)^2$.

Quasicrystals in three dimensions

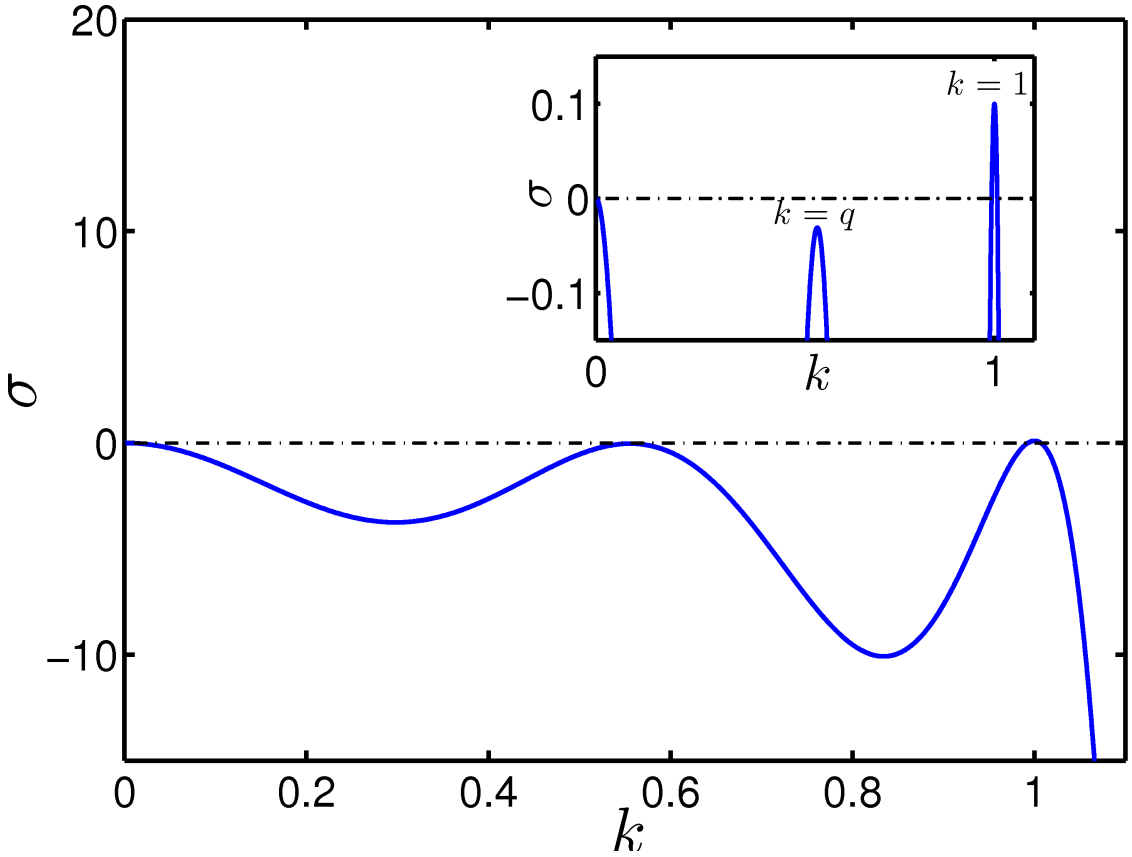

Growth rate $\sigma(k)$ as a function of the wavenumber k for the linear operator $\mathcal{L}$ with parameters $\sigma_0 = -100$, $q = 1/\tau = 0.6180$, $\mu = 0.1$ and $\nu = -0.1$. The growth rates at $k = 1$ and $k = q$ are μ and $q^2\nu$, as in the inset.

Quasicrystals in three dimensions

Density perturbation waves (at one length scale) of the form $e^{i\mathbf{k}\cdot\mathbf{x}}$ with wavevectors chosen to be the 30 edge vectors of an icosahedron can take advantage of three-wave interactions (from the triangular faces) and of five-wave interactions (from the pentagons surrounding five triangular faces) to lower the free energy and so encourage the formation of icosahedral QCs. With two length scales in the golden ratio τ, an alternative mechanism for reinforcing icosahedral symmetry is possible using only three-wave interactions. We take five edge vectors of a pentagon adding up to zero, eg. $\mathbf{k}_{16} + \mathbf{k}_7 + \mathbf{k}_{15} + \mathbf{k}_2 + \mathbf{k}_{25} = 0$, such that $\mathbf{k}_7 + \mathbf{k}_{15} = \mathbf{q}_2$ and $\mathbf{k}_2 + \mathbf{k}_{25} = \mathbf{q}_4$, resulting in a three-wave interaction between $\mathbf{q}_2$, $\mathbf{q}_4$ and $\mathbf{k}_{16}$.

j	$\mathbf{k}_j$	j	$\mathbf{k}_j$	j	$\mathbf{k}_j$
1	$(1,0,0)$	6	$\frac{1}{2}(1,\tau-1,\tau)$	11	$\frac{1}{2}(\tau-1,\tau,-1)$
2	$\frac{1}{2}(\tau,1,\tau-1)$	7	$\frac{1}{2}(1,\tau-1,-\tau)$	12	$\frac{1}{2}(\tau-1,-\tau,-1)$
3	$\frac{1}{2}(\tau,1,1-\tau)$	8	$\frac{1}{2}(1,1-\tau,-\tau)$	13	$\frac{1}{2}(\tau-1,-\tau,1)$
4	$\frac{1}{2}(\tau,-1,1-\tau)$	9	$\frac{1}{2}(1,1-\tau,\tau)$	14	$(0,1,0)$
5	$\frac{1}{2}(\tau,-1,\tau-1)$	10	$\frac{1}{2}(\tau-1,\tau,1)$	15	$(0,0,1)$

Quasicrystals in three dimensions

We now use a weakly nonlinear theory, with $U = \epsilon U_1$, with μ and ν chosen such that $\mathcal{L} = O(\epsilon^3)$. We also take $Q = \epsilon Q_1$. For icosahedral QCs, we use the vectors from the Table and expand U_1 as

$$U_1 = \sum_{j=1}^{15} z_j \, e^{i\mathbf{k}_j \cdot \mathbf{x}} + \sum_{j=1}^{15} w_j \, e^{i\mathbf{q}_j \cdot \mathbf{x}} + \text{c.c.} + \text{h.o.t.}$$

Thus the rescaled volume-specific free energy $f = \mathcal{F}/(V\epsilon^4)$ is

$$\begin{aligned} f = & - \mu z_1 \bar{z}_1 - 4Q_1 \big(w_{10} z_4 - w_{11} z_5 - w_{12} z_2 - w_{13} z_3 \\ & \qquad - w_3 w_5 - w_2 w_4 - z_6 z_8 - z_7 z_9 \big) \bar{z}_1 \\ & - \mu \sum_{j=2}^{15} |z_j|^2 - \nu \sum_{j=1}^{15} |w_j|^2 \\ & - Q_1 (152 \text{ other cubic terms}) - (1305 \text{ quartic terms}). \end{aligned}$$

The evolution of the amplitudes z_j, w_j is thus governed by the equations

$$\dot{z}_j = -\frac{\partial f}{\partial \bar{z}_j} \qquad \text{and} \qquad \dot{w}_j = -q^2 \frac{\partial f}{\partial \bar{w}_j}.$$

Quasicrystals in three dimensions

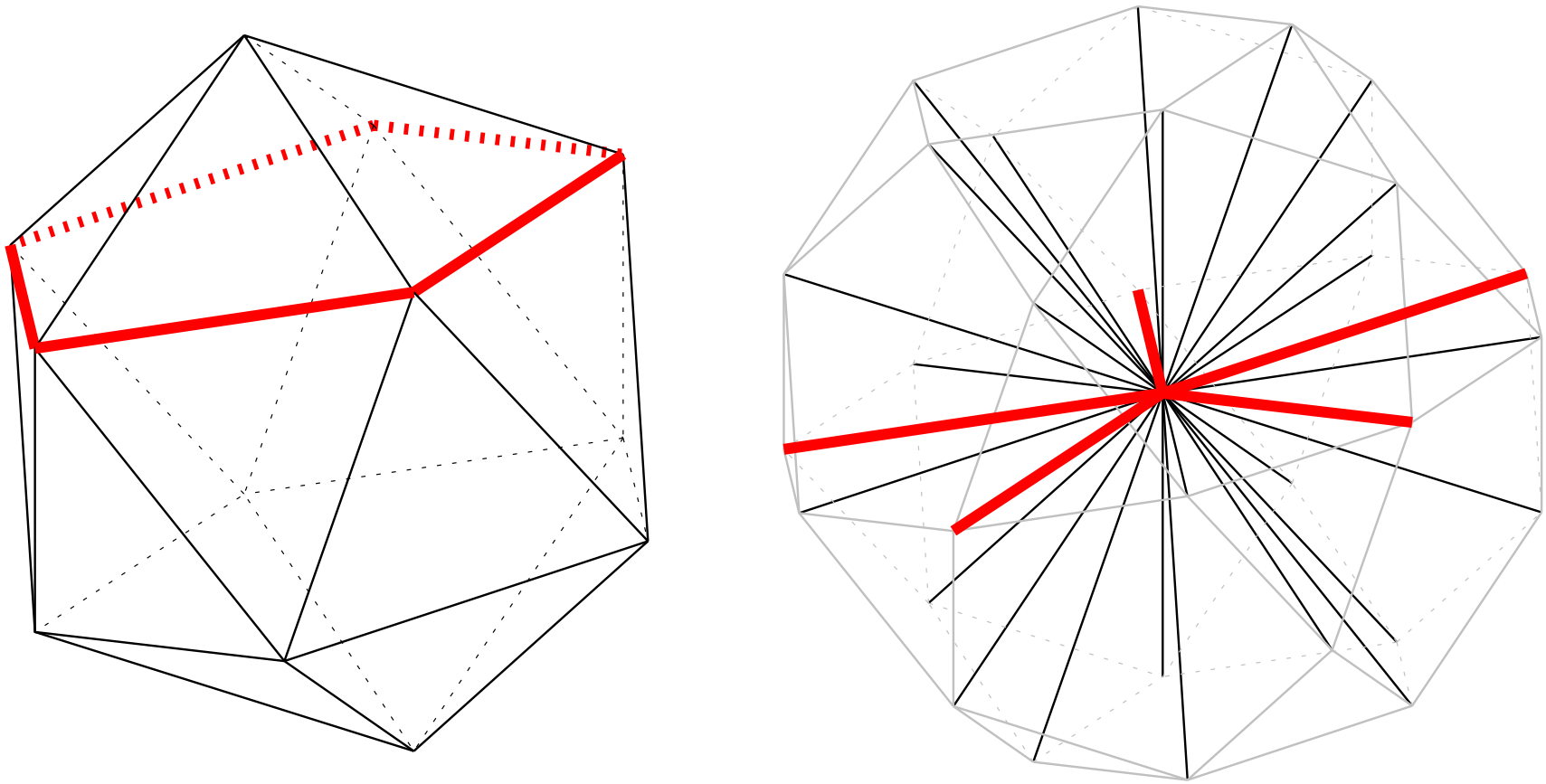

(a) An icosahedron and (b) an icosidodecahedron showing the five wavevectors (red) that sum to zero.

Crystalline phases in three dimensions

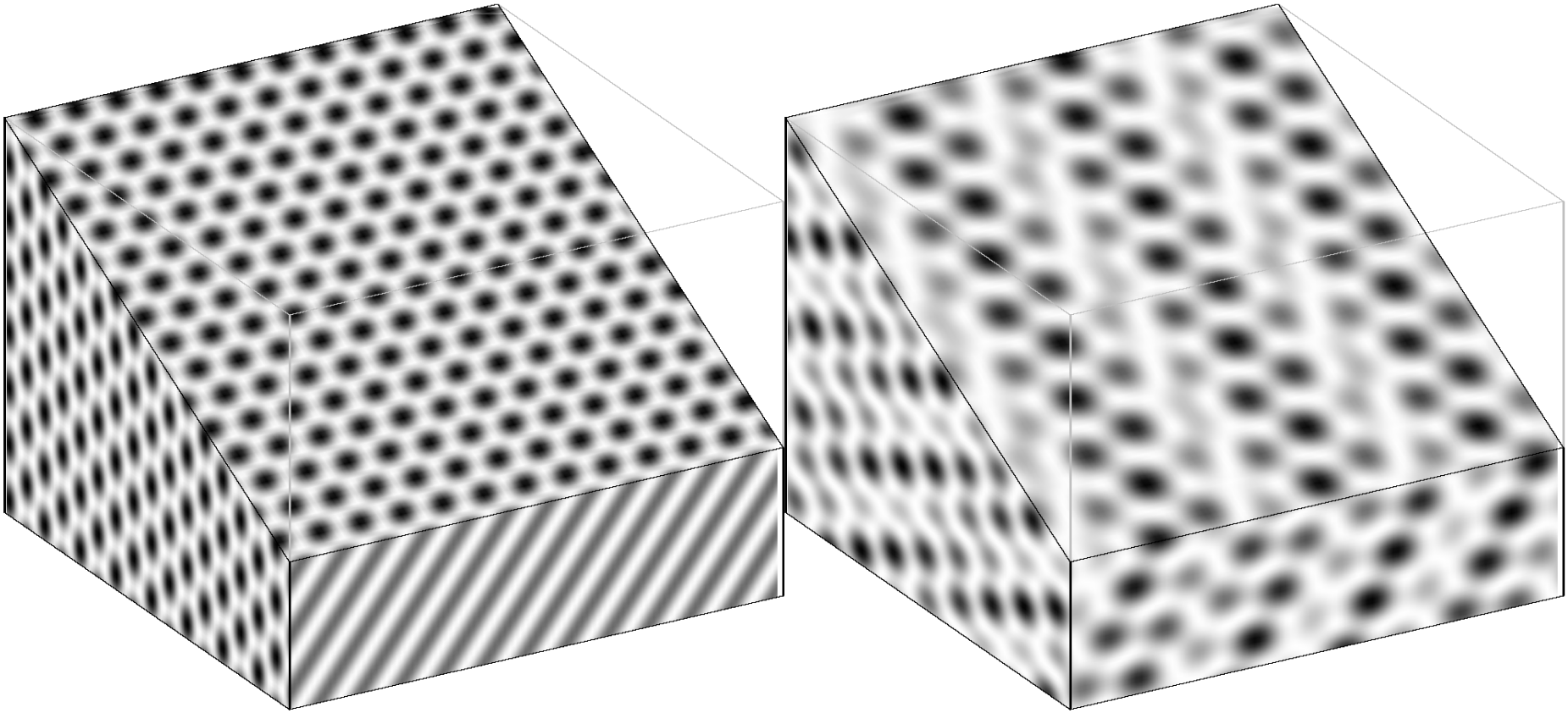

(a) Hexagonal columnar phase with wavenumber q (q-hex) at $(\mu, \nu) = (0.082, 0.056)$. (b) Body centered cubic crystal with wavenumber 1 (1-bcc) at $(\mu, \nu) = (-0.1, 0)$.

Quasicrystals in three dimensions

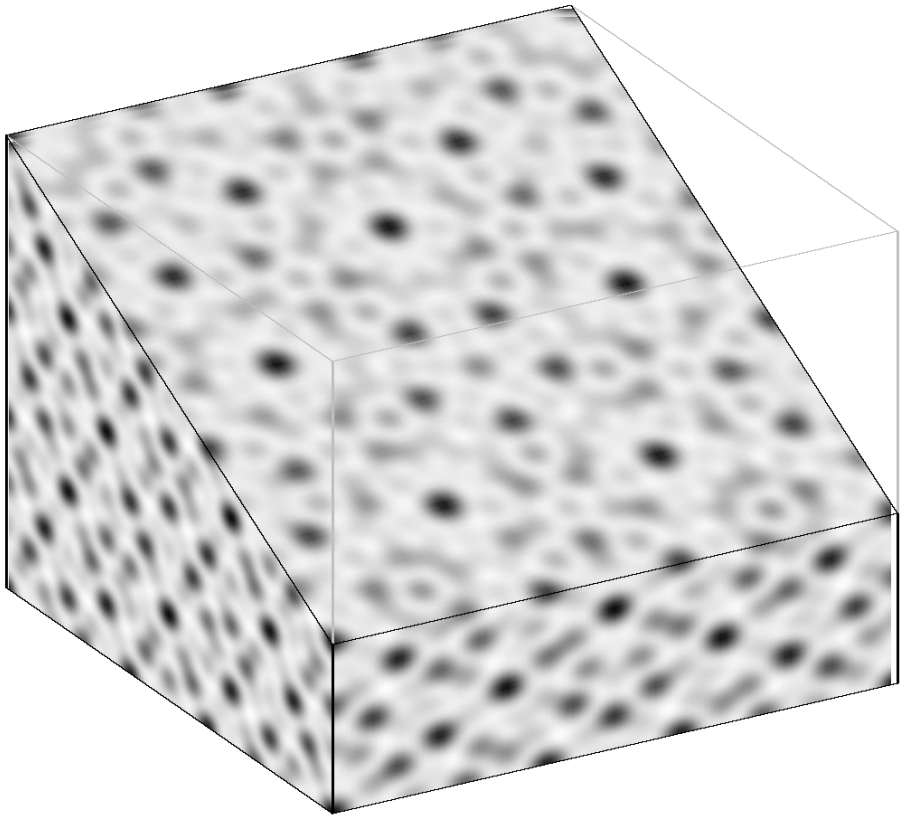

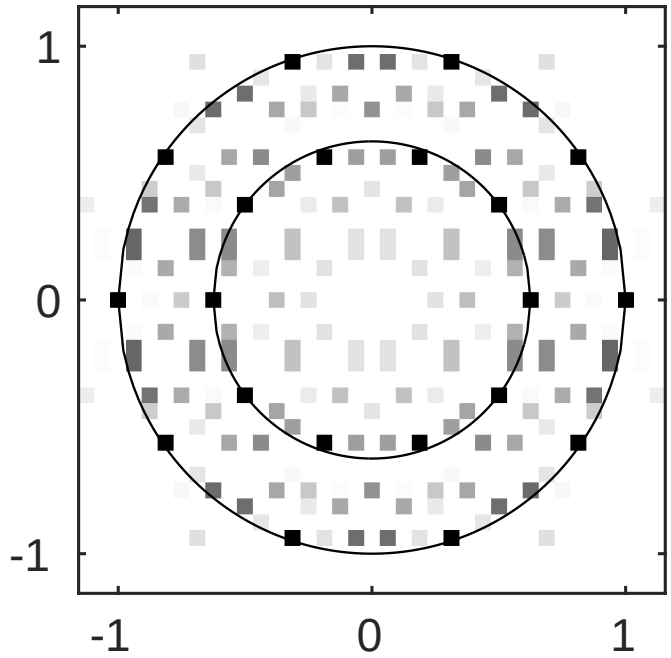

(a) Icosahedral quasicrystal (QC) at $(\mu, \nu) = (-0.071, -0.071)$. Each box has had a slice cut away, chosen to reveal the 5-fold rotation symmetry.
(b) Diffraction pattern taken in a plane normal to the vector $(\tau, -1, 0)$ in Fourier space. The circles of radii 1 and q are indicated. Domain: $16\lambda \times 16\lambda \times 16\lambda$.

Quasicrystals in three dimensions

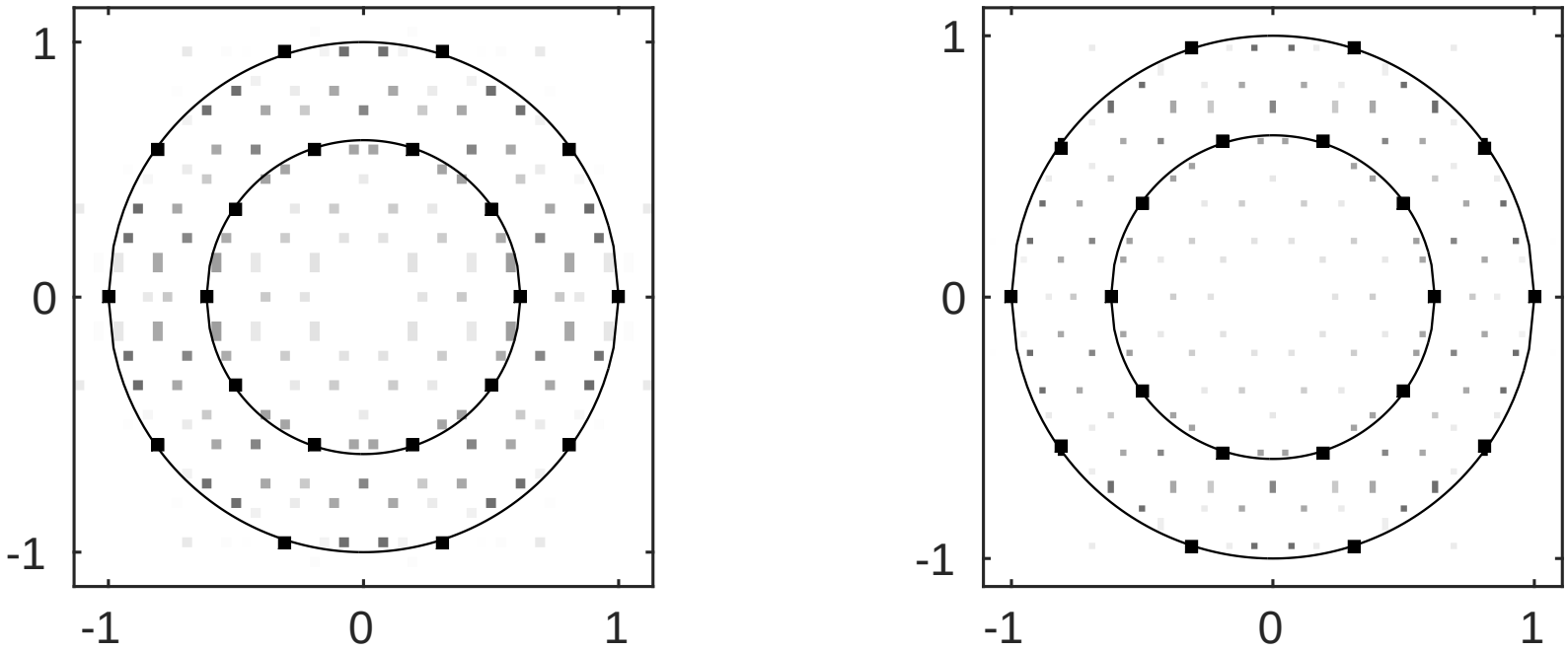

Diffraction patterns obtained from (a) a $26\lambda \times 26\lambda \times 26\lambda$ and (b) a $42\lambda \times 42\lambda \times 42\lambda$ calculation.

Quasicrystals in three dimensions

The big question now is whether the 3D quasicrystals constructed in this way are **stable**.

We calculate the minimum free energy f associated with each class of solutions (both crystal and quasicrystal), at each point (μ, ν) in parameter space. By minimizing f over all solution classes at a given (μ, ν), we identify the globally stable solution at that state point. Body-centered cubic (bcc) crystals cannot be represented in terms of the icosahedral basis vectors, and we compute their free energy in a separate calculation, choosing a different set of basis vectors.

The next figure shows the results.

Quasicrystals in three dimensions

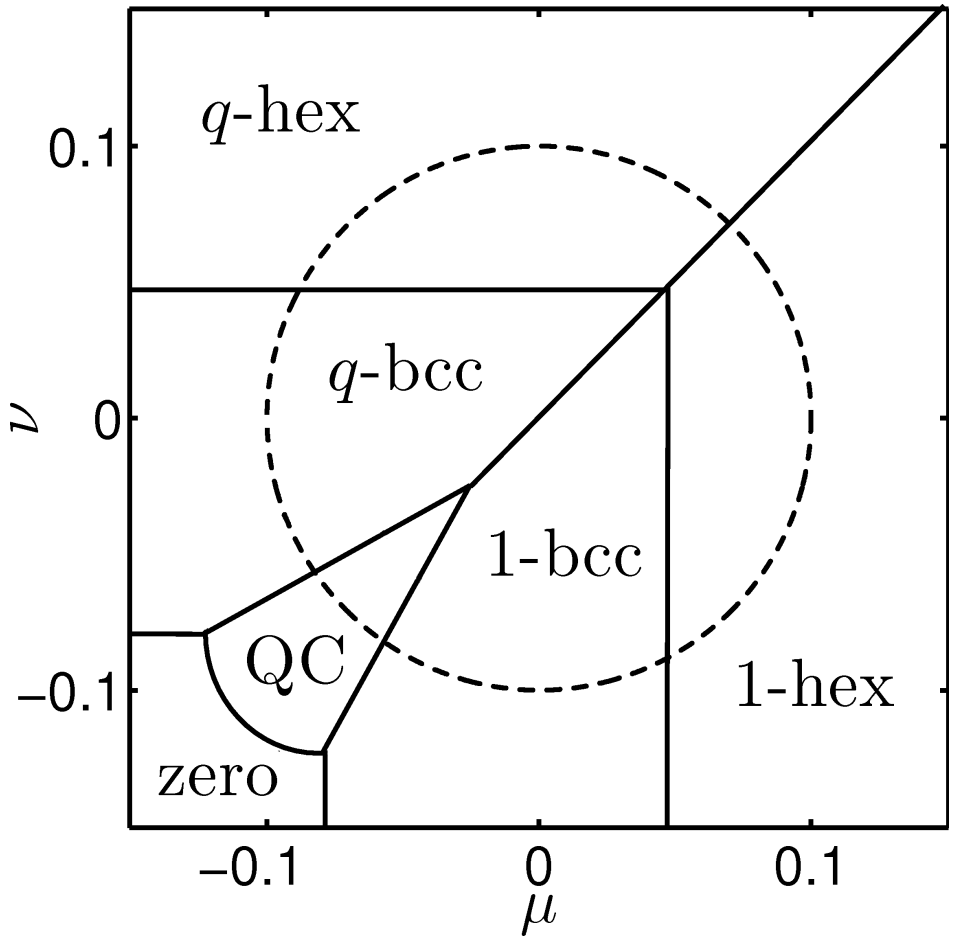

Structures with minimal specific free energy f over a range of parameters μ and ν, computed from the amplitude equations. PDE calculations are performed on the dashed circle around the origin with radius 0.1. The region 'zero' indicates that the trivial state $U = 0$ is globally stable.

Quasicrystals in three dimensions

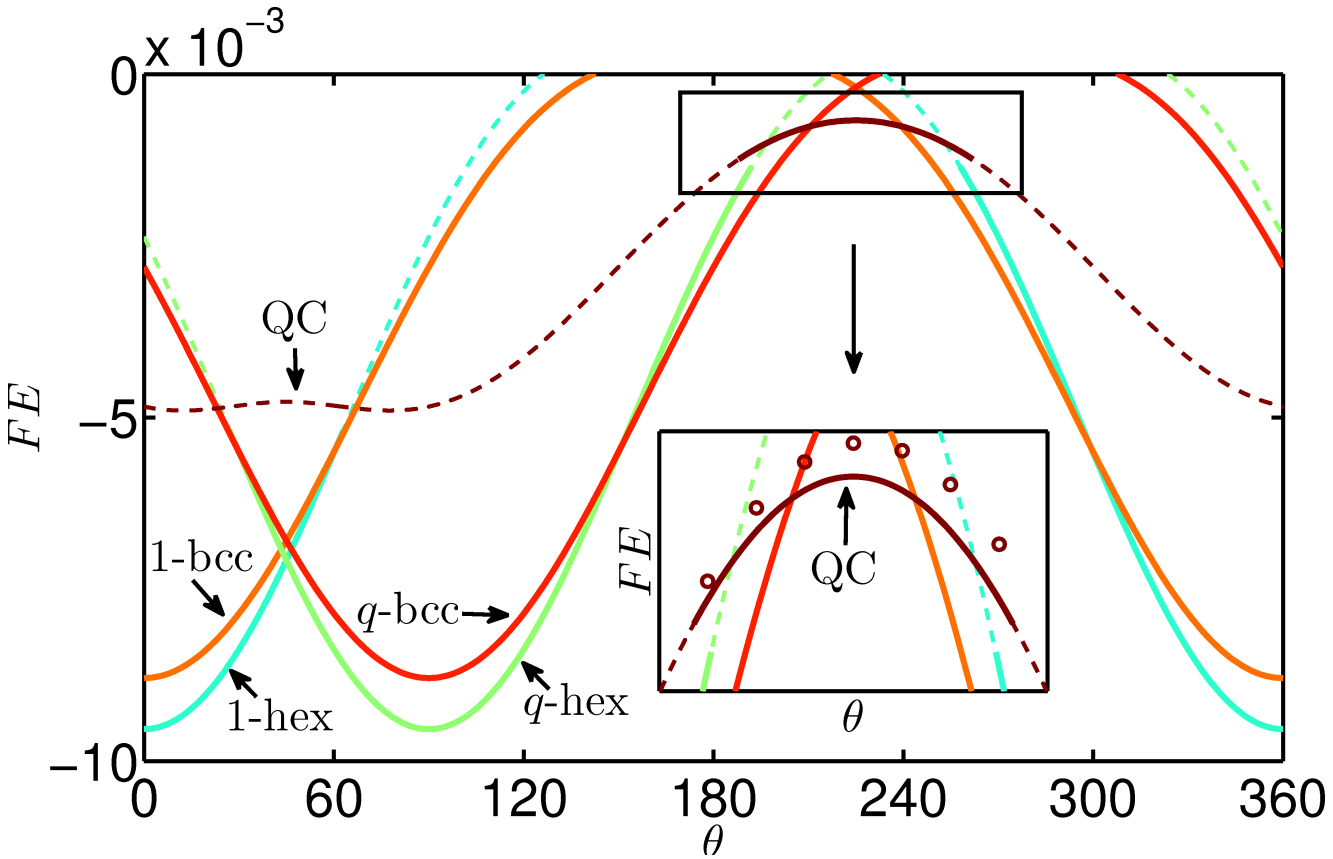

Variation of specific free energy f with angle θ on a circle in the (μ, ν) plane of radius 0.1. Lines track the variation of free energy f of the labeled structures (solid: locally stable, dashed: locally unstable). The stability of the bcc crystals cannot be compared directly with that of QCs. Hollow circles show the free energies of locally stable quasicrystalline asymptotic steady states from PDE

Quasicrystals in three dimensions

(a)

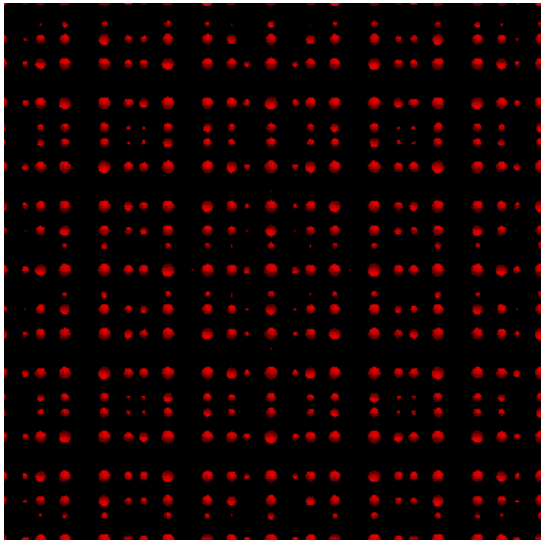

(b)

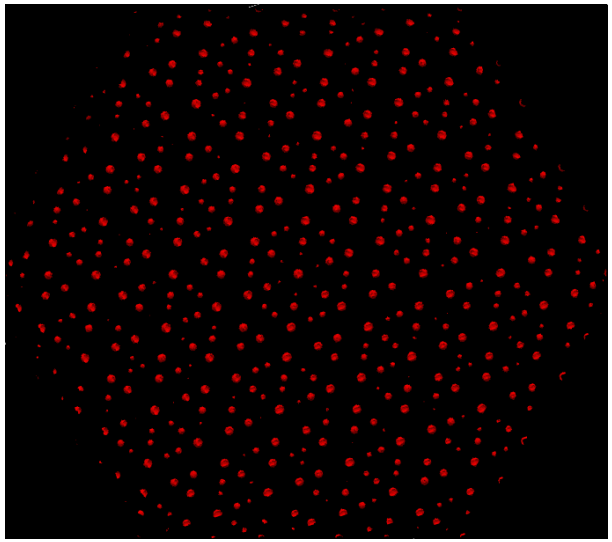

(c)

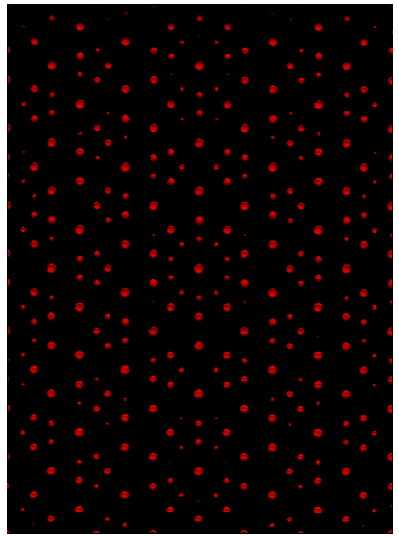

Parallel projections of the contour cloud along the high symmetry directions. (a) 2-fold symmetry observed in a plane perpendicular to $(1, 0, 0)$. (b) 3-fold symmetry observed in a plane perpendicular to $(-1, 1, 1)$. (c) 5-fold symmetry observed in a plane perpendicular to $(\tau, -1, 0)$.

Localized quasicrystals in two dimensions

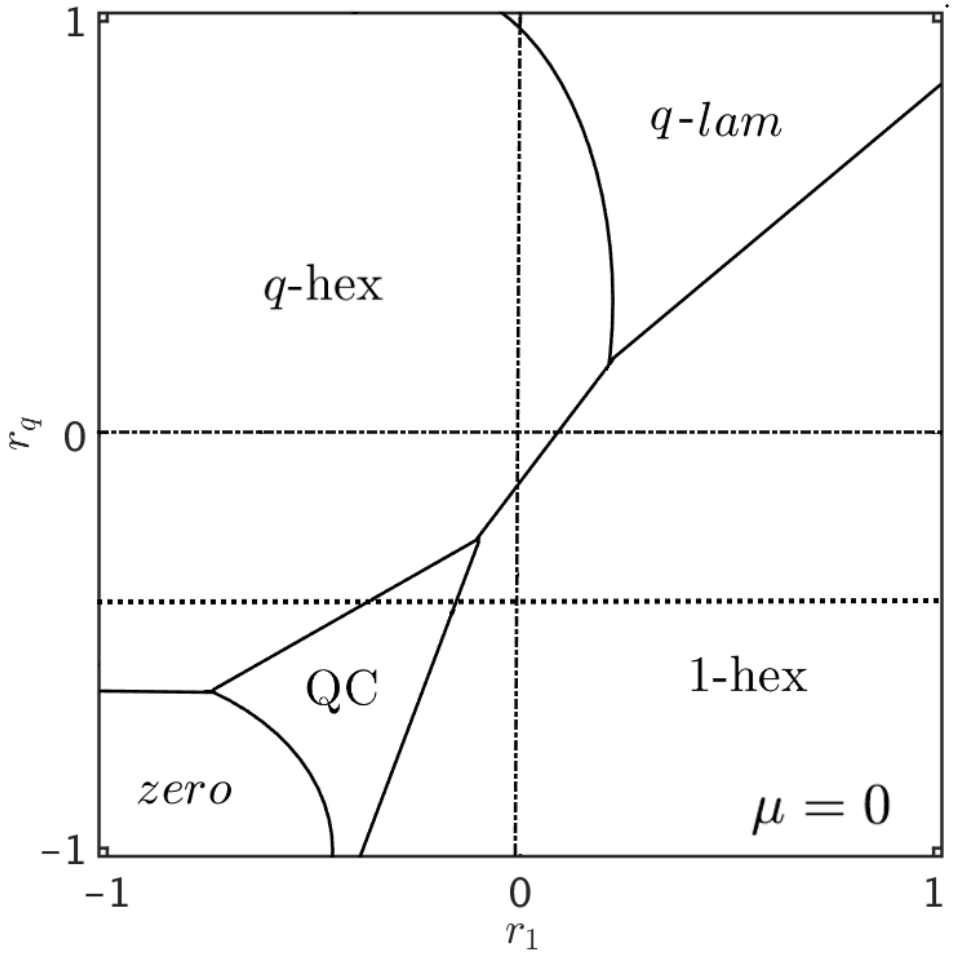

Thermodynamically stable structures in the (r_1, r_q) plane, computed as global minima of the grand potential Ω for the chemical potential $\mu = 0$. Dashed-dotted lines indicate the axes while the dotted line indicates variation of r_1 for the choice of $r_q = -0.412$ which we explore in detail.

Localized quasicrystals in two dimensions

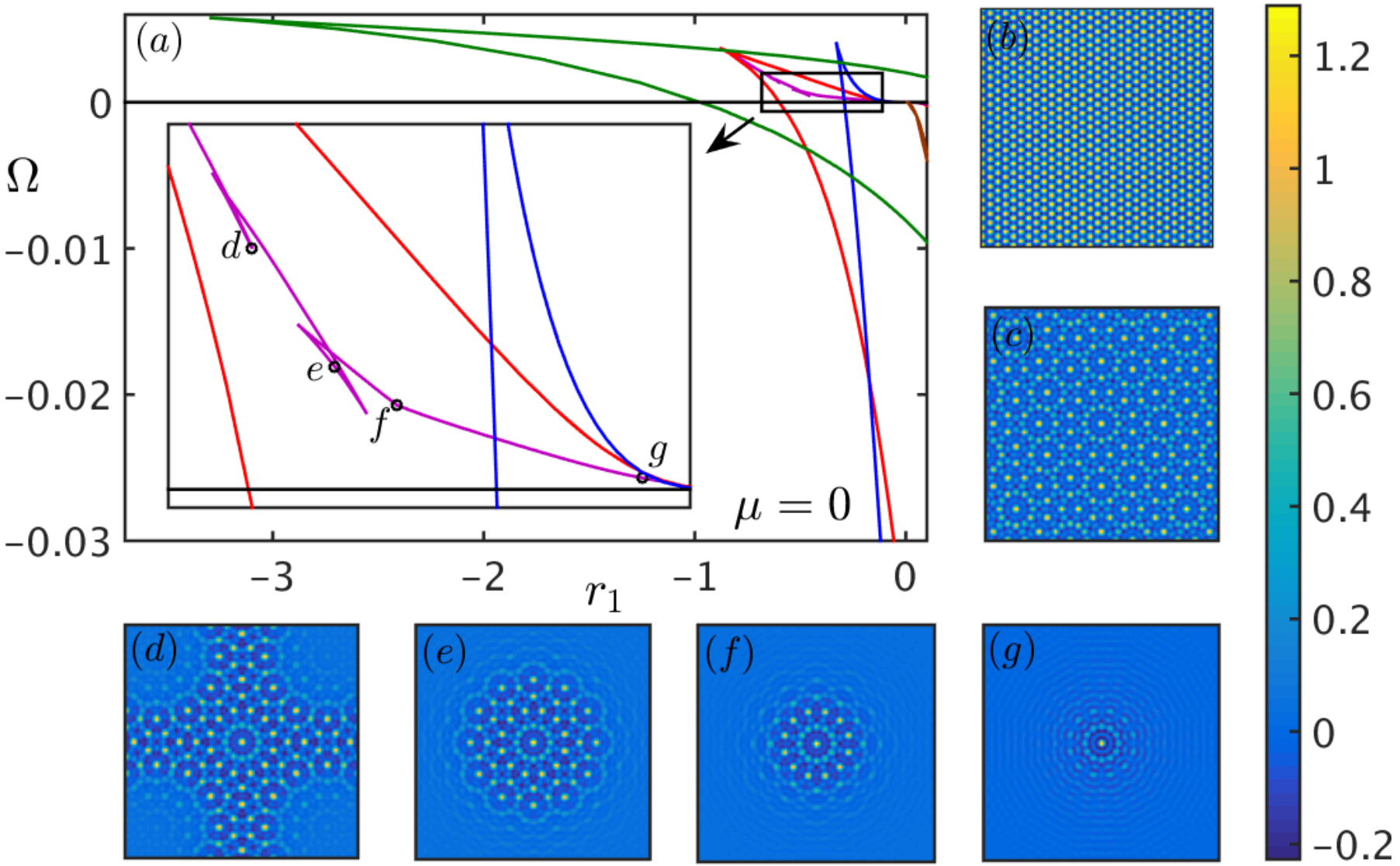

(*a*) Grand potential Ω as a function of the linear growth rate r_1 for $r_q = -0.412$, $\mu = 0$. Blue line: 1-hexagons, green: q-hexagons, red: QC, magenta: LQC.

Localized quasicrystals in two dimensions

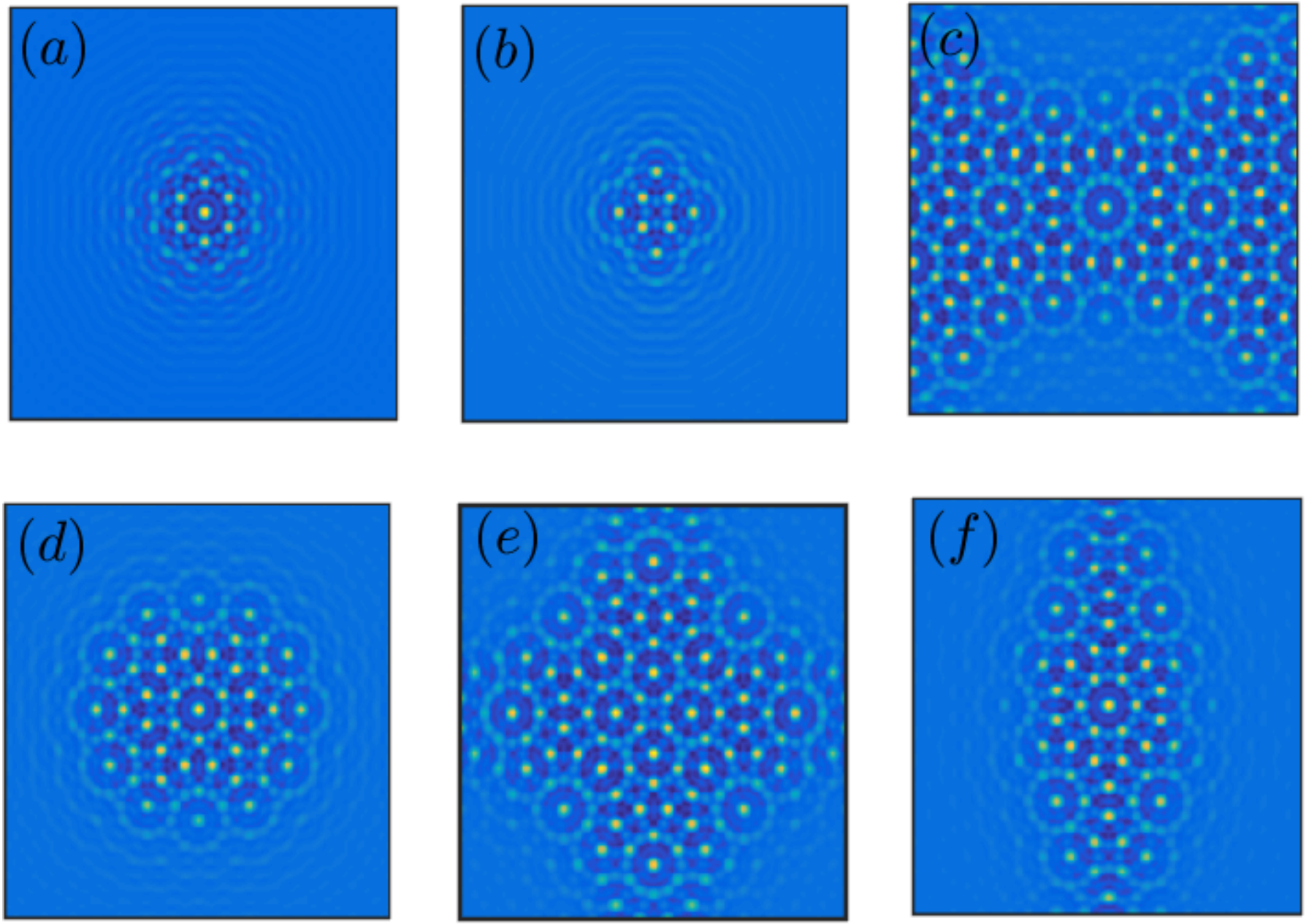

Localized quasicrystals in two dimensions

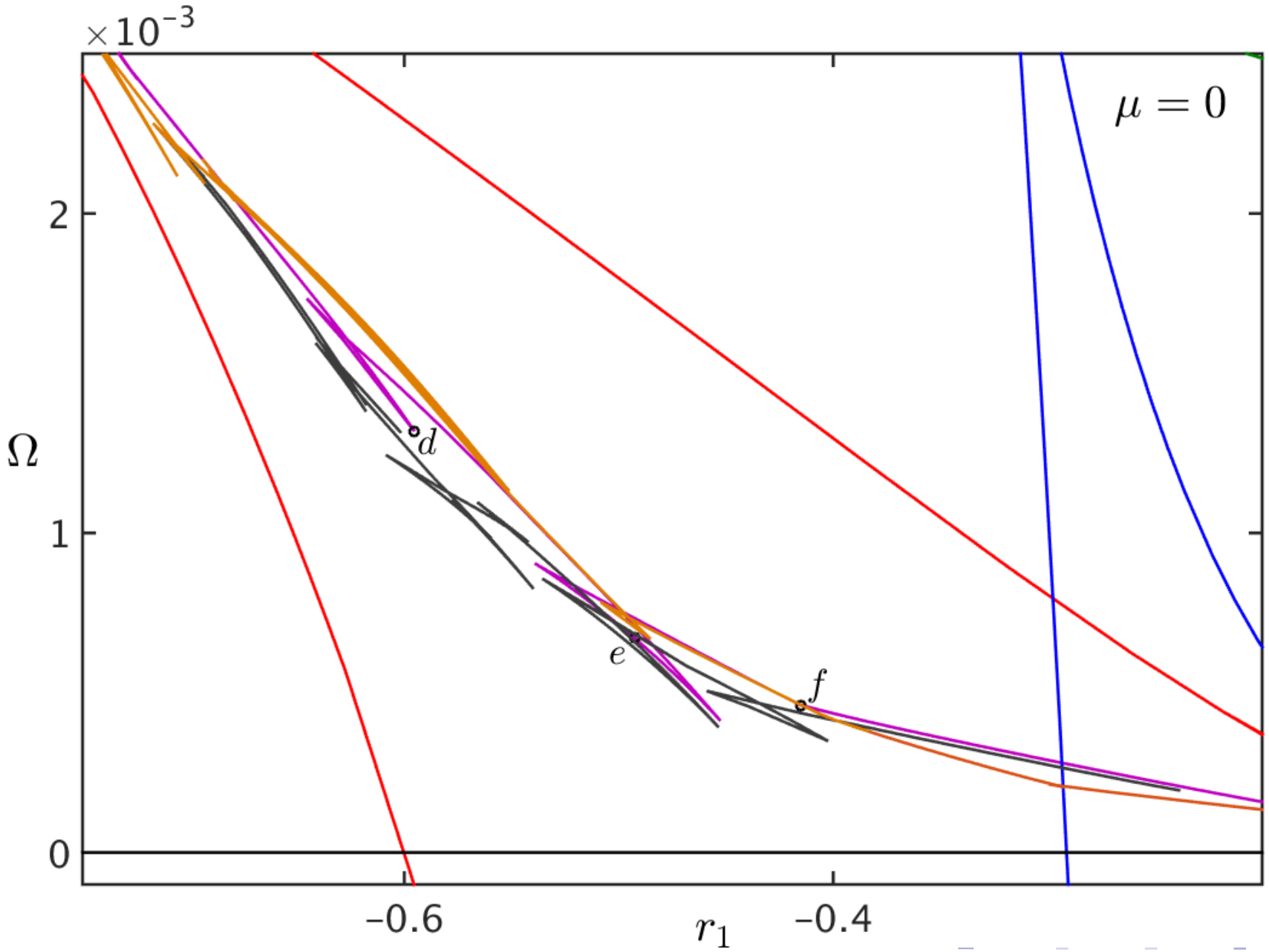

Localized quasicrystals in three dimensions

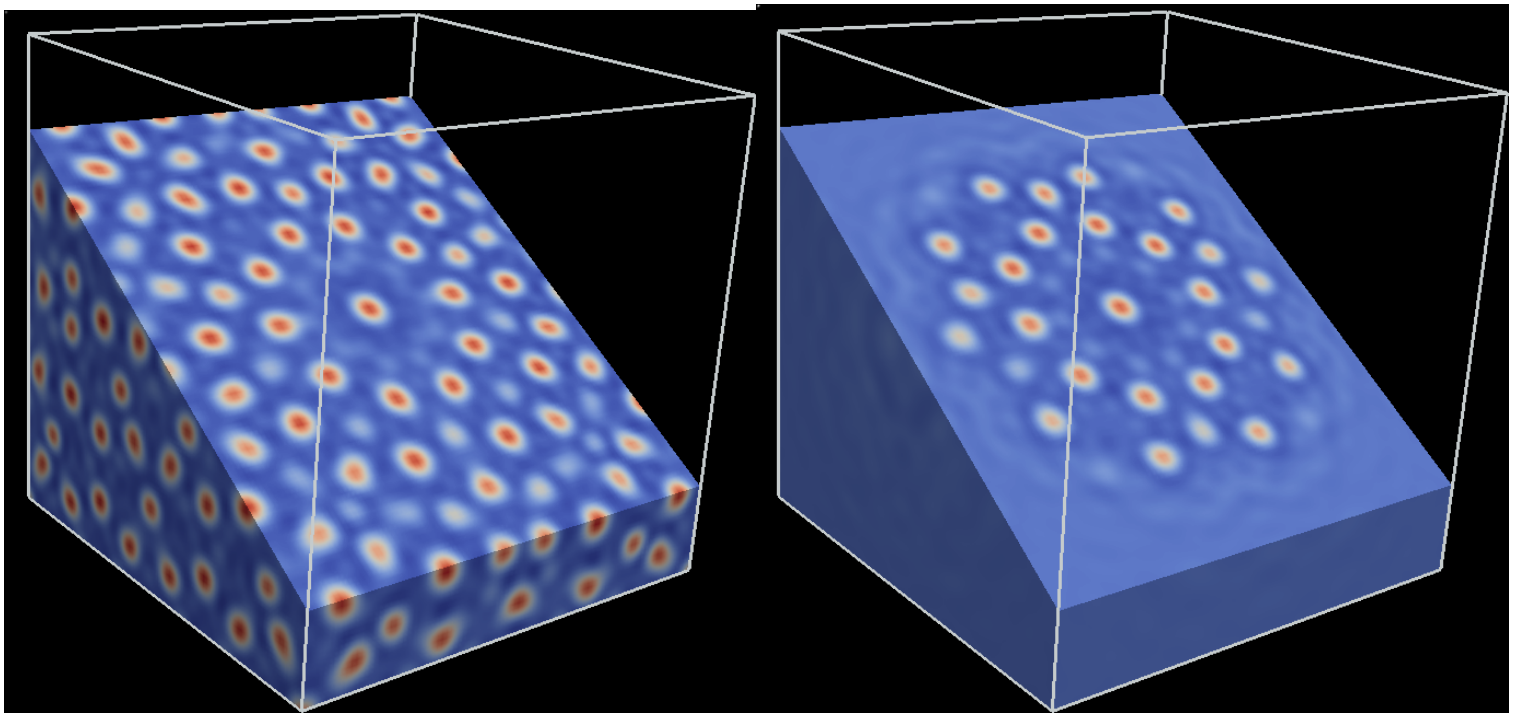

Variation of the scalar density U in 3D sliced along the plane $(\tau, 0, 1)$ where $\tau = 1.618$ for (a) an extended icosahedral quasicrystal and (b) a dynamically stable localized quasicrystal at the same parameters of $r_1 = -0.51$, $r_q = -0.51$, $q = 0.618$, $Q = 2$, $\sigma = -10$ and $\mu = 0$.

Localized quasicrystals in two dimensions

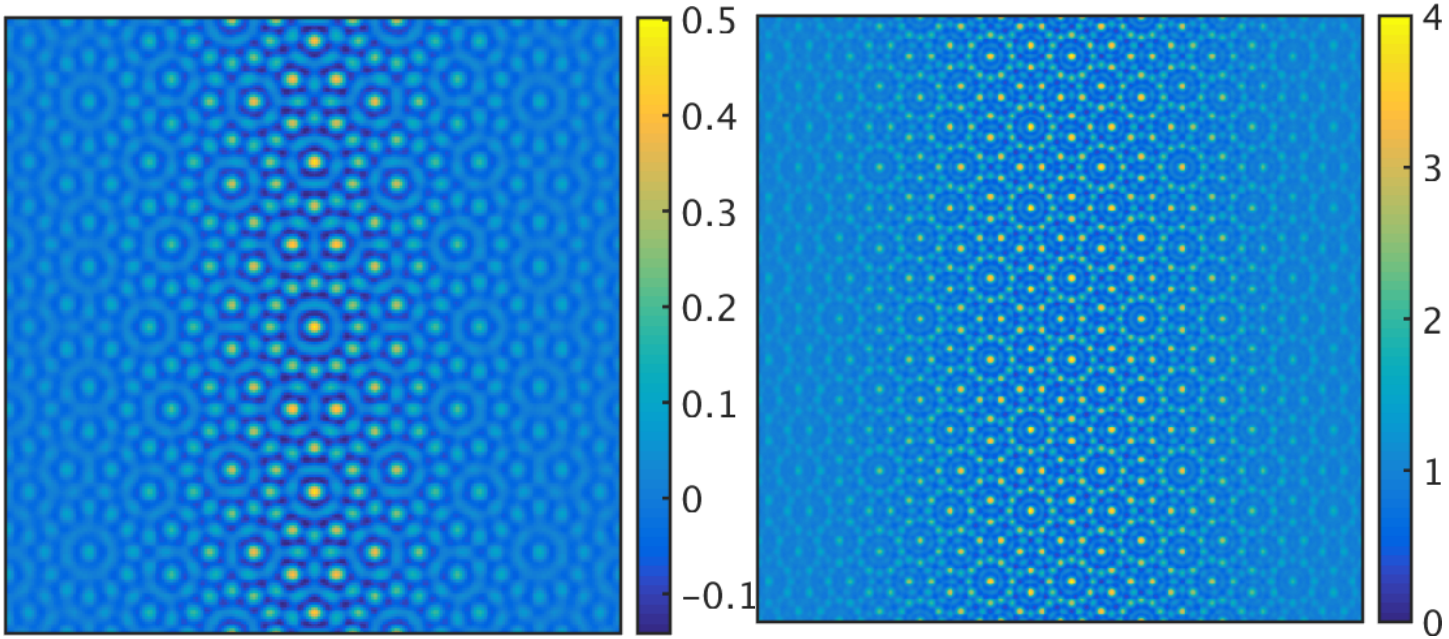

(a) Spatial variation of scalar density U showing a 1D localized state of quasicrystal in the PFC model at parameters $r_1 = -0.1152$, $r_q = -0.412$, $q = 0.5176$, $\sigma = -10$ and $Q = 2$, (b) Spatial variation of density ρ in a DFT model with pair potential as defined in Barkan et al. (2011) with potential $v(r) = 10\, e^{-0.5*(0.770746*r)^2} \left(1.0 - 1.09r^2 + 0.4397r^4 - 0.05r^6 + 0.002r^8\right)$ showing 1D localization of a quasicrystalline state similar to (a).

Conclusions

We have discussed the properties of soft matter systems in 2D and 3D using simple models for particle-particle interaction exhibiting **two** scales

- In 2D a generalization of the GEM-8 model leads to the formation of metastable quasicrystals with 12-fold symmetry. These states are obtained both via Picard iteration and in Brownian dynamics particle simulations. The two scales may be excited linearly or nonlinearly.
- In 3D we used the simpler PFC model with two scales to demonstrate the existence of an icosahedral quasicrystal that is a global free energy minimum and hence thermodynamically **stable**.
- Localized quasicrystals bifurcate from the QC branch and may serve as nuclei in a two-step nucleation process.

A.J. Archer, A.M. Rucklidge and E. Knobloch, Phys. Rev. Lett. **111**, 165501 (2013) and Phys. Rev. E **92**, 012324 (2015);
P. Subramanian, A.J. Archer, A.M. Rucklidge and E. Knobloch, Phys. Rev. Lett. **117**, 075501 (2016) and paper in preparation